PHILOSOPHICAL TRANSACTIONS OF THE ROYAL SOCIETY A MATHEMATICAL, PHYSICAL & ENGINEERING SCIENCES

The Distribution of the Magnetic Field and Return Current Round a Submarine Cable Carrying Alternating Current. Part 2

S. Butterworth

Phil. Trans. R. Soc. Lond. A 1924 **224**, 141-184
doi: 10.1098/rsta.1924.0004

IV.—*The Distribution of the Magnetic Field and Return Current round a Submarine Cable carrying Alternating Current.—Part 2.*

By S. Butterworth, *M.Sc., Admiralty Research Laboratory, Teddington.*

Communicated by F. E. Smith, *F.R.S.*

(Received April 4,—Read May 31, 1923.)

[Plates 1–4.]

1. *Introduction.*

The following theory of the distribution of magnetic field above a submarine cable carrying alternating currents was developed at the suggestion of the Admiralty, and the experimental verification of the theory by means of a model was carried out at the Admiralty Research Laboratory, Teddington. The results are published by permission of the Admiralty. I have also been allowed to make use of the results obtained by Dr. C. V. Drysdale in a research carried out on the Gareloch in order to compare the theory with measurements made on the sea. In 1897 Mr. C. S. Whitehead* published a theory giving the effect of a plane conducting sheet on the field due to a circular current. His results, however, are not in accord with experiment, and it may be shown that his mathematical analysis is unsound. More recently M. Abraham† has determined the distribution of current stream lines in a thin conducting sheet due to various sources of alternating current. His results, however, do not cover the present case.

I. Theoretical.

2. *General Equations for Field due to a Submarine Cable.*

Take the vertical line through the cable as the axis of y and a line on the bed of the sea perpendicular to the cable as the axis of x (fig. 1). Let D be the depth of the sea

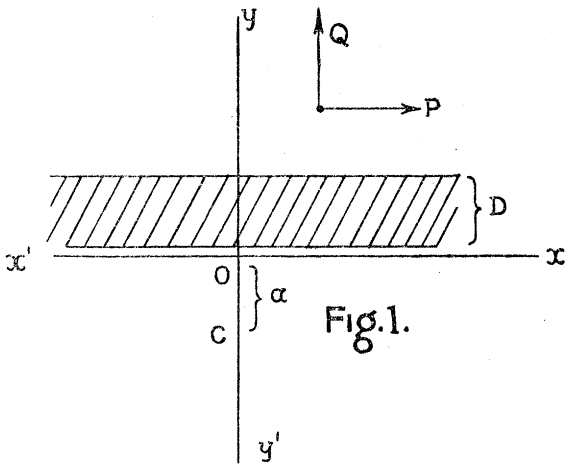

Fig. 1.

* 'Phil. Mag.,' vol. 44, p. 154 (1897).

† 'Zeit. Math. u. Mechanik,' vol. 2, p. 109 (1922).

and suppose at first that the cable is buried at a depth a below the sea bed. Then if E be the rotor representing the induced electric force parallel to the cable, P, Q the rotors representing the horizontal and vertical components of the magnetic field, we have from the electromagnetic relations

$$\frac{\partial E}{\partial x} = j\omega Q, \qquad \frac{\partial E}{\partial y} = -j\omega P, \qquad \frac{\partial Q}{\partial x} - \frac{\partial P}{\partial y} = 4\pi k E \quad . \quad . \quad . \quad . \quad . \quad . \quad (1)$$

in which k is the conductivity of the sea, $\omega/2\pi$ the frequency (f) of the alternating current in the cable and j is the operator rotating through a right angle.

Eliminating P, Q

$$\frac{\partial^2 E}{\partial x^2} + \frac{\partial^2 E}{\partial y^2} = \Lambda^2 E \quad . \quad . \quad . \quad . \quad . \quad . \quad . \quad . \quad . \quad . \quad . \quad . \quad (2)$$

in which

$$\Lambda^2 = 4\pi k\omega j = 8\pi^2 j/L^2 \text{ say} \quad . \quad . \quad . \quad . \quad . \quad . \quad . \quad . \quad . \quad . \quad . \quad . \quad (3)$$

Here L^2 is written for $1/kf$ so that L represents the wave-length of electromagnetic waves of frequency f in an unlimited ocean of conductivity k.

In the present problem, E must have even symmetry about the axis of y and must therefore be capable of expression as the sum of normal solutions of (2) of the type.

$$E_m = (B\epsilon^{-m'y} + C\epsilon^{m'y}) \cos mx \quad . \quad . \quad . \quad . \quad . \quad . \quad . \quad . \quad . \quad . \quad . \quad . \quad (4)$$

where m is a variable parameter,

$$m'^2 = m^2 + \Lambda^2$$

and B and C are functions of m.

Since E is finite at all points above the sea and since $\Lambda = 0$ above and below the sea the appropriate normal solutions to use are

(a) $y = D$ to $y =$ infinity,

$$E_m = A\epsilon^{-my} \cos mx \quad . \quad . \quad . \quad . \quad . \quad . \quad . \quad . \quad . \quad . \quad . \quad . \quad (5)$$

(b) $y = 0$ to $y = D$,

$$E_m = (B\epsilon^{-m'y} + C\epsilon^{m'y}) \cos mx \quad . \quad . \quad . \quad . \quad . \quad . \quad . \quad . \quad . \quad . \quad . \quad . \quad (6)$$

(c) y negative,

$$E_m = (B'\epsilon^{-my} + C'\epsilon^{my}) \cos mx. \quad . \quad . \quad . \quad . \quad . \quad . \quad . \quad . \quad . \quad . \quad . \quad . \quad (7)$$

The five functions A, B, C, B′, C′ are not independent as there are four boundary conditions to satisfy, viz. :—E, $\partial E/\partial y$ are continuous both at $y = 0$ and $y = D$. These conditions lead to the following equations expressing A, B, C, C′ in terms of B′ :—

$$\left.\begin{aligned} \frac{A}{B} &= \frac{4mm'\epsilon^{mD}}{\Delta}, & \frac{C'}{B'} &\equiv \frac{2\Lambda^2 \sinh m'D}{\Delta} \\ \frac{B}{B'} &= \frac{2m(m'+m)\epsilon^{m'D}}{\Delta}, & \frac{C}{B'} &= \frac{2m(m'-m)\epsilon^{-m'D}}{\Delta} \end{aligned}\right\} \quad . \quad . \quad . \quad . \quad . \quad (8)$$

$$\Delta = (m'+m)^2 \epsilon^{m'D} - (m'-m)^2 \epsilon^{-m'D} \quad . \quad . \quad . \quad . \quad . \quad . \quad . \quad . \quad . \quad . \quad . \quad (9)$$

We have still to determine the form of B′ suitable for the present problem.

If the conductivity of the sea were zero, equations (8) would give

$$C = C' = 0, \qquad A = A' = B'$$

so that the electric force would be expressed by

$$E_m = B' \epsilon^{-my} \cos mx \quad \ldots\ldots\ldots\ldots (10)$$

at all points.

(10) is therefore the form of the *undisturbed* electric force giving rise to the system (5), (6) and (7) when the sea is of finite conductivity. To find B′, the *undisturbed* distribution due to the cable must be expressed as a series of which the general term is of the type (10). Now the magnetic field due to a long cable carrying current I_0 (and flowing from the observer) has components

$$P = \frac{2I_0 (a+y)}{(a+y)^2 + x^2}, \qquad Q = \frac{-2I_0 x}{(a+y)^2 + x^2} \quad \ldots\ldots\ldots (11)$$

at any point x, y in fig. 1.

These expressions may be written

$$\left.\begin{aligned} P &= 2I_0 \int_0^\infty \epsilon^{-m(a+y)} \cos mx\, dm \\ Q &= -2I_0 \int_0^\infty \epsilon^{-m(a+y)} \sin mx\, dm \end{aligned}\right\} \quad \ldots\ldots\ldots (11a)$$

so that by (1) the field components are derived from an electric force

$$E = 2j\omega I_0 \int_0^\infty \epsilon^{-m(a+y)} \cos mx\, dm/m \quad \ldots\ldots\ldots (12)$$

The integrand in this expression must be identical with (10) so that

$$B' = 2j\omega I_0 \epsilon^{-ma}\, dm/m \quad \ldots\ldots\ldots\ldots (13)$$

Writing down the corresponding values of A, B, C from (8), inserting in (5) and (6) and integrating from 0 to infinity we have for the electric force due to a cable at a depth a below the bed of the sea,

(a) above the surface of the sea

$$E = 8j\omega I_0 \int_0^\infty m' \epsilon^{-m(a+y-D)} \cos mx\, dm/\Delta \quad \ldots\ldots\ldots (14)$$

(b) below the surface of the sea

$$E = E_1 + E_2$$

in which

$$\left.\begin{aligned} E_1 &= 4j\omega I_0 \int_0^\infty (m' + m)\, \epsilon^{-ma} \epsilon^{m'(D-y)} \cos mx\, dm/\Delta \\ E_2 &= 4j\omega I_0 \int_0^\infty (m' - m)\, \epsilon^{-ma} \epsilon^{-m'(D-y)} \cos mx\, dm/\Delta \end{aligned}\right\} \quad \ldots\ldots (15)$$

It is seen from (14) that if a be diminished and y increased by the same amount, the electric force is unaltered. In the corresponding case of a non-magnetic conducting plate this change is equivalent to a motion of translation of the plate. Anticipating a result to be obtained in Section 3 it may be asserted that a rotatory motion of the plate about an axis parallel to the cable will merely alter the direction of the field acting at a fixed point on the far side of the plate provided that the distance between point and cable be not too small.

Hence in shielding apparatus from the disturbing effects of a system of parallel cables, the position of the plate is immaterial so far as screening efficiency is concerned.

Field above the Surface of the Sea.

3. *Field at Large Distances from the Cable.*

Suppose the cable is situated on the bed of the sea and let the origin of co-ordinates be transferred to the surface point (O, D). Then (14) becomes

$$\mathrm{E} = 8j\omega \mathrm{I}_0 \int_0^\infty m' \epsilon^{-my} \cos mx \, dm/\Delta. \quad \ldots\ldots\ldots \quad (16)$$

Now although the integration with respect to m extends to infinity we may for large values of y regard m as small because of the factor ϵ^{-my} in the integral. Neglecting m in Δ/m' we have $\Delta/m' \doteqdot 2\Lambda \sinh \Lambda \mathrm{D}$ and

$$\mathrm{E} = \frac{4j\omega \mathrm{I}_0}{\Lambda \sinh \Lambda \mathrm{D}} \int_0^\infty \epsilon^{-my} \cos mx \, dm = \frac{4j\omega \mathrm{I}_0}{\Lambda \sinh \Lambda \mathrm{D}} \frac{y}{x^2 + y^2} = \frac{4j\omega \mathrm{I}_0}{\Lambda \sinh \Lambda \mathrm{D}} \frac{\cos \theta}{r} \quad (17)$$

where $r^2 = x^2 + y^2$, $\tan \theta = x/y$.

Again whether y be large or not E satisfies Laplace's equation, has even symmetry about the axis of y, and vanishes as r approaches infinity. Hence E must always be of the form $\mathrm{E}_1 \cos \theta/r + \mathrm{E}_2 \cos 2\theta/r^2 + \ldots$ settling down to $\mathrm{E}_1 \cos \theta/r$ when r is large. It may therefore be asserted that the result (17) holds for large values of r even for points on the surface of the sea.

The values of the components of magnetic field corresponding to (17) are

$$\mathrm{P} = \frac{4\mathrm{I}_0}{\Lambda \sinh \Lambda \mathrm{D}} \frac{\cos 2\theta}{r^2}, \qquad \mathrm{Q} = -\frac{4\mathrm{I}_0}{\Lambda \sinh \Lambda \mathrm{D}} \frac{\sin 2\theta}{r^2} \quad \ldots\ldots \quad (18)$$

These values are such as would be produced by a vertical current doublet of moment $2\mathrm{I}_0/\Lambda \sinh \Lambda \mathrm{D}$ situated at the surface of the sea. The lines of force at distant points are arcs of circles having their centres on the y axis and all passing through the origin so that the angle which the field makes with the horizontal at any point is double the horizontal angle of the radius vector drawn to the point. The amplitude and phase of the field are given by the formula

$$\mathrm{H} = 4\mathrm{I}_0/\Lambda r^2 \sinh \Lambda \mathrm{D} \qquad \text{in which} \qquad \Lambda^2 \mathrm{D}^2 = 8\pi^2 j \mathrm{D}^2/\mathrm{L}^2 = 2j\gamma^2 \text{ (say)} \quad \ldots \quad (19)$$

When ΛD is small

$$H \doteqdot 4I_0/\Lambda^2 Dr^2 = -2jI_0 D/\gamma^2 r^2 = -jH_0 D/r\gamma^2 \quad \ldots\ldots\ldots (20)$$

where H_0 is the undisturbed field $(2I_0/r)$. Thus the field is in quadrature with the current and its amplitude is obtained by multiplying the undisturbed field by $D/r\gamma^2 \equiv L/4\pi^2 Dr$.

For moderate values of ΛD (20) must be multiplied by $\Lambda D/\sinh \Lambda D$, the amplitude of which is $U = 2\gamma(\cosh 2\gamma - \cos 2\gamma)^{\frac{1}{2}}$ and the lagging phase $\tan^{-1}(\cosh \gamma \tan \gamma) - \frac{\pi}{4}$. Thus if

$$\frac{\gamma}{2\pi} = \frac{D}{L} = \quad \tfrac{1}{8} \qquad \tfrac{1}{4} \qquad \tfrac{3}{8} \qquad \tfrac{1}{2} \qquad \tfrac{3}{4} \qquad 1$$

$$U = 0{\cdot}995 \quad 0{\cdot}887 \quad 0{\cdot}631 \quad 0{\cdot}383 \quad 0{\cdot}120 \quad 0{\cdot}033.$$

Equation (20) may therefore be used with fair accuracy if $D/L < 0{\cdot}2$.

When ΛD is large

$$H = 8I_0 \epsilon^{-\Lambda D}/\Lambda r^2 = 4\sqrt{2} I_0 D \epsilon^{-\gamma} \epsilon^{-j\left(\gamma + \frac{\pi}{4}\right)}/\gamma r^2 \quad \ldots\ldots\ldots (21)$$

The field amplitude is now $2\sqrt{2} I_0 L \epsilon^{-2\pi D/L}/\pi r^2$ and the lagging phase $\pi(2D/L + \frac{1}{4})$.

4. *Range of Distant Field Formulæ.*

If we expand m'/Δ as far as m^2, substitute in (16) and integrate we find

$$E = \frac{4j\omega I_0}{\Lambda \sinh \Lambda D}\left[\frac{\cos\theta}{r} - \frac{2 \coth \Lambda D \cos 2\theta}{\Lambda r^2} - \frac{\{3 + \coth \Lambda D(\Lambda D - 8)\}\cos 3\theta}{\Lambda^2 r^3}\right]. \quad (22)$$

For small values of ΛD the coefficients of the FOURIER series are

$$\frac{1}{r}, \qquad \frac{2}{\Lambda^2 Dr^2}, \qquad \frac{8}{\Lambda^3 Dr^3}$$

or in terms of wave-lengths the *amplitudes* of these coefficients are as

$$1 : L^2/4\pi^2 Dr : 2\sqrt{2}\pi D/L\,(L^2/4\pi^2 Dr)^2. \quad \ldots\ldots\ldots (23)$$

If the second term is small so also will be the third as D/L is small. Hence when D/L is small the distant field formula will hold if $L^2/4\pi^2 Dr$ is small. Since, however, the second term has an imaginary coefficient, the first effect of diminishing distance is on the *phase* of E. We may make $L^2/4\pi^2 Dr$ as great as $0{\cdot}1$ before the amplitude of E departs appreciably from that given by the first term. For 1 per cent. accuracy in amplitude r must be greater than $L^2/4D$. For large values of ΛD the coefficients are

$$\frac{1}{r}, \qquad \frac{2}{\Lambda r^2}, \qquad \frac{D}{\Lambda r^3}.$$

Thus if the depth is large the third term may be as important as the second.

The limiting distance is now given by $1/\Lambda r$ small and the limiting depth by $D < 2r$. The former condition will hold to 5 per cent. if r exceeds 3 wave-lengths. The criteria for the application of the distant field formulæ are therefore

$$\left.\begin{array}{llll} D/L & \text{small} & r > L^2/4D & \\ D/L & \text{large} & r > 3L, & D < 2r \end{array}\right\} \quad \ldots\ldots\ldots \quad (24)$$

5. *Field above the Sea at Low Frequencies.—The Lamina Theory.*

Let the following substitutions be made in equation (14)

$$y = sD, \quad x = tD, \quad \Lambda^2 D^2 = k, \quad mD = \xi, \quad m'D = \xi', \quad w = s + it^* \quad \ldots \quad (25)$$

so that

$$\xi'^2 = \xi^2 + k \quad \ldots\ldots\ldots\ldots\ldots \quad (26)$$

Then

$$E = 4j\omega I_0 \int_0^\infty \epsilon^{-\xi s} \cos \xi t \, . \, d\xi/F = \text{real part}^* \; 4j\omega I_0 \int_0^\infty \epsilon^{-\omega\xi} \, d\xi/F. \quad \ldots \quad (27)$$

in which

$$F = \{(\xi' + \xi)^2 \, \epsilon^{\xi' - \xi} - (\xi' - \xi)^2 \, \epsilon^{\xi' + \xi}\}/2\xi'. \quad \ldots\ldots\ldots \quad (28)$$

Since at low frequencies D/L is small, k is small, so F will be expanded in ascending powers of k yielding

$$F = 2\xi + k + \tfrac{1}{4}k^2 \left(\frac{1}{\xi} - \frac{1}{\xi^2} + \frac{1 - \epsilon^{-2\xi}}{\xi^3}\right) + \ldots. \quad \ldots\ldots\ldots \quad (29)$$

The last recorded term in the series is merely to be used to estimate the error involved in ignoring this and succeeding terms. The coefficient of k^2 may therefore be replaced by its maximum value which occurs when $\xi = 0$ and is then equal to $\frac{1}{6}$. With this assumption we may write

$$F = 2\xi + k + \tfrac{1}{6}k^2 \quad \ldots\ldots\ldots\ldots\ldots \quad (30)$$

or

$$\frac{1}{F} = \frac{1}{2\xi + k} - \frac{k^2}{6(2\xi + k)^2}. \quad \ldots\ldots\ldots\ldots\ldots \quad (31)$$

Inserting in (27)

$$E = \text{real part } 4j\omega I_0 \left(y_1 + \tfrac{1}{6}k^2 \frac{dy_1}{dk}\right) \quad \ldots\ldots\ldots \quad (32)$$

in which

$$y_1 = \int_0^\infty \frac{\epsilon^{-w\xi} \, d\xi}{2\xi + k} \quad \ldots\ldots\ldots\ldots\ldots \quad (33)$$

Now using the substitutions $2\xi = -juk$, $w\xi = qu$ so that by (25) and (3)

$$q = 4\pi^2 D \, (y + ix)/L^2 = \beta + i\alpha \text{ say} \quad \ldots\ldots\ldots \quad (34)$$

* *Note.*—i represents a "space" rotation and j a "time" rotation. "Real part" is in regard to complex quantities involving "i."

we obtain

$$y_1 = \tfrac{1}{2}\int_0^\infty \frac{\epsilon^{-qu}}{u+j}\,du = -\tfrac{1}{2}\left(\frac{d\mathrm{G}}{dq} + j\mathrm{G}\right), \quad \ldots\ldots\ldots \quad (35)$$

in which

$$\mathrm{G} = \int_0^\infty \frac{\epsilon^{-qu}}{1+u^2}\,du. \quad \ldots\ldots\ldots\ldots \quad (36)$$

Also

$$\tfrac{1}{6}k^2\frac{dy_1}{dk} = \tfrac{1}{3}j\,\frac{q^2}{w}\frac{dy_1}{dq}$$

and

$$\frac{dy_1}{dq} = -\tfrac{1}{2}\left(\frac{d^2\mathrm{G}}{dq^2} + j\frac{d\mathrm{G}}{dq}\right) = -\tfrac{1}{2}\left(\frac{1}{q} - \mathrm{G} + j\frac{d\mathrm{G}}{dq}\right) = -\frac{1}{2q} + jy_1.$$

Hence the last term of (32) is by (19)

$$\tfrac{1}{6}j\,\frac{q}{w} - \tfrac{1}{3}\frac{q^2}{w}y_1 = \gamma^2\,(\tfrac{1}{6}j - \tfrac{1}{3}qy_1). \quad \ldots\ldots\ldots\ldots \quad (37)$$

To the order of the approximation we now have

$$\mathrm{E} = \text{real part} - 2j\omega\mathrm{I}_0\left\{\left(\frac{d\mathrm{G}}{dq} + j\mathrm{G}\right)(1 - \tfrac{1}{3}\gamma^2 q) + \tfrac{1}{3}j\gamma^2\right\}, \quad \ldots\ldots \quad (38)$$

or if the last term be ignored

$$\mathrm{E} = (-)\,2j\omega\mathrm{I}_0\,(\mathrm{G}'_{\mathrm{R}} + j\mathrm{G}_{\mathrm{R}}). \quad \ldots\ldots\ldots\ldots \quad (39)$$

The components of magnetic field follow by differentiation using (1).

Remembering that

$$\frac{\partial \mathrm{E}}{\partial y} = -i\frac{\partial \mathrm{E}}{\partial x} = \frac{\gamma^2}{\mathrm{D}}\frac{\partial \mathrm{E}}{\partial q},$$

we have

$$\left.\begin{aligned} \mathrm{P} &= \text{real part}\ \ \frac{2\mathrm{I}_0\gamma^2}{\mathrm{D}}\left(\frac{1}{q} - \mathrm{G} + j\mathrm{G}'\right) \\ \mathrm{Q} &= \text{imag. part}\ \frac{2\mathrm{I}_0\gamma^2}{\mathrm{D}}\left(\frac{1}{q} - \mathrm{G} + j\mathrm{G}'\right) \end{aligned}\right\} \quad \ldots\ldots\ldots \quad (40)$$

Thus the electric force and field components are defined in terms of the single function G given by (36).

Since the undisturbed field is given by

$$\mathrm{P}_0 + i\mathrm{Q}_0 = 2\mathrm{I}_0\gamma^2/\mathrm{D}q \quad \ldots\ldots\ldots\ldots \quad (41)$$

equation (40) shows that the phases and amplitudes of the ratios of the modified and undisturbed field components are functions only of the two variables β and α of equations (34). If these quantities are plotted on a single diagram with α and β as co-ordinates, this diagram may be made to represent a space diagram at any frequency, conductivity, or depth (within the prescribed limits) by mere adjustment of scale, unit length in space being represented by $2\pi k\omega\mathrm{D}$ on the α, β diagram. See Charts 1, 2, 3, 4 (Plates 1 and 2).

The approximate results (39) and (40) would have also been obtained if we had replaced the sea by a lamina of infinitely large conductivity and infinitely small depth, the product of conductivity and depth being finite and equal to that for the sea.

For brevity the results deduced from (39) and (40) will be referred to as those obtained by the lamina theory.

6. *Formulæ for the Evaluation of G (q) and G′ (q).*

The function G is defined as a definite integral in (36). By differentiating twice with respect to q we find $G'' = 1/q - G$, so that all the differential coefficients of G may be expressed in terms of G and G′.

When q is real ($= \beta$), (36) may be converted into sine and cosine integrals, giving

$$\left.\begin{aligned} G(\beta) &= \sin\beta\, Ci(\beta) + \cos\beta\left\{\frac{\pi}{2} - Si(\beta)\right\} \\ G'(\beta) &= \cos\beta\, Ci(\beta) - \sin\beta\left\{\frac{\pi}{2} - Si(\beta)\right\} \end{aligned}\right\} \quad \ldots\ldots\ldots (42)$$

Now the sine and cosine integrals $Si(\beta)$, $Ci(\beta)$ are tabulated* so that (42) may be used to compute the field vertically above the cable. (See Table II. of Appendix.)

Also when q is imaginary ($= i\alpha$)

$$\left.\begin{aligned} G_R(i\alpha) &= \frac{\pi}{2}\epsilon^{-\alpha} = G'_I(i\alpha) \\ G_I(i\alpha) &= \tfrac{1}{2}\{\epsilon^{\alpha} Ei(-\alpha) - \epsilon^{-\alpha} Ei(\alpha)\} \\ G'_R(i\alpha) &= \tfrac{1}{2}\{\epsilon^{\alpha} Ei(-\alpha) + \epsilon^{-\alpha} Ei(\alpha)\} \end{aligned}\right\} \quad \ldots\ldots\ldots (43)$$

the subscripts denoting real and imaginary parts, and $Ei(\alpha)$, $Ei(-\alpha)$ being the exponential integrals.

These formulæ have been used to compute the field on the surface of the lamina. (Table III.)

When q is complex no tables are available. However if $|q|$ is not too large, the following series (derived from the exponential integral series) may be used—

$$G(q) = \frac{\pi}{2}\cos q + (\log q - 0{\cdot}422784)\sin q + \left(\frac{q}{10}\right)^3 f_3 - \left(\frac{q}{10}\right)^5 f_5 + \left(\frac{q}{10}\right)^7 f_7 - , \quad (44)$$

$$G'(q) = 1 + (\log q - 0{\cdot}422784)\cos q - \frac{\pi}{2}\sin q + \left(\frac{q}{10}\right)^2 f_2 - \left(\frac{q}{10}\right)^4 f_4 + \ldots, \quad (45)$$

in which

$$f_n = \frac{10^n}{\lfloor n}\left(\tfrac{1}{2} + \tfrac{1}{3} + \ldots + \frac{1}{n}\right).$$

* Glaisher, 'Phil. Trans.,' vol. 160, pp. 367–387 (1870). Dale's Tables, pp. 85 and 86.

From these formulæ Tables IV., V., VI., VII., have been computed, giving the values of the field components in directions inclined at angles 0, 15, 30, 45, 60, 75, 90 degrees to the vertical with values of R ($\equiv \sqrt{\beta^2 + \alpha^2}$) ranging from 1 to 10.

7. *Charts embodying Results of Lamina Theory.*

If horizontal traverses were made measuring the in-phase and quadrature components of the horizontal and vertical magnetic field in the air above the cable, curves could be drawn connecting these components with horizontal distance x for various values of vertical distance y. These curves could be employed to construct four surfaces or models in which the co-ordinates would be x, y, and the field component in question. Such a set would be required for every combination of frequency and depth. If, however, we measured each field component in terms of the undisturbed field at the same height vertically over the cable (viz., in terms of $P_0 = 2I_0/y$) and replaced the co-ordinates x, y by $\alpha = 4\pi^2 Dx/L^2$, $\beta = 4\pi^2 Dy/L^2$, then the lamina theory shows that if D/L is not too large, all the models corresponding to a given field component should be alike, so that only four models are necessary.

Charts 1, 2, 3, 4 give the plans of these models as predicted by the lamina theory. They have been constructed from Tables IV.–VII. by graphical interpolation. Chart I. gives the lines P_R/P_0 constant where P_R is the in-phase component, of the horizontal field. Over the cable, P_R/P_0 falls continually from unity. The line $P_R = 0$ tends asymptotically to the line $\tan^{-1} \alpha/\beta = \pi/6$ and there is a maximum negative value of P_R/P_0 of amount 0·09 when $\alpha = 1{\cdot}42$, $\beta = 0{\cdot}50$.

Chart 2 gives the lines P_I/P_0 = constant, P_I being the quadrature component of the field. Over the cable P_I/P_0 rises to a maximum negative value 0·35 when $\beta = 0{\cdot}8$ and then falls continuously. There is a small maximum positive value at the point $\alpha = 3{\cdot}8$, $\beta = 1{\cdot}25$. The line $P_I = 0$ tends asymptotically towards the line $\tan^{-1} \alpha/\beta = \pi/4$.

In Chart 3, the maximum value of Q_R/P_0 for horizontal traverses occurs along the line a, tending asymptotically towards the line $\tan^{-1} \alpha/\beta = \pi/8$. A secondary maximum of opposite sign occurs along the line b tending towards $\tan^{-1} \alpha/\beta = 3\pi/8$, while the line $Q_R = 0$ tends towards $\tan^{-1} \alpha/\beta = \pi/3$.

In Chart 4, the line c represents the locus of the maximum values of Q_I/P_0 for horizontal traverses. The line c is identical with the line $P_R = 0$ in Chart 1.

8. *Lamina Theory at Large Distances.*

For points vertically above the cable, the value of G (β) when β is large is determined as follows :—

$$G(\beta) = \int_0^\infty \frac{e^{-\beta u}\, du}{1 + u^2}.$$

Now the integrand is always positive and the value of $1/(1+u^2)$ is alternately less and greater than

$$1, \qquad 1-u^2, \qquad 1-u^2+u^4, \quad \text{etc.}$$

Hence the true value of G (β) is alternately less and greater than

$$\frac{1}{\beta}, \qquad \frac{1}{\beta}-\frac{\lfloor 2}{\beta^3}, \qquad \frac{1}{\beta}-\frac{\lfloor 2}{\beta^3}+\frac{\lfloor 4}{\beta^5}, \quad \text{etc.},$$

so that when β is large, G (β) approximates to $1/\beta$.

Similarly G′ (β) approximates to $-1/\beta^2$.

Therefore by (39)

$$E = 2\omega I_0/\beta. \qquad \ldots\ldots\ldots\ldots\ldots\ldots \quad (46)$$

For points not on the vertical we obtain from the same argument as in Section (3),

$$E = 2\omega I_0 \cos\theta/R \qquad \ldots\ldots\ldots\ldots\ldots\ldots \quad (47)$$

where

$$R^2 = \alpha^2+\beta^2, \qquad \tan\theta = \alpha/\beta.$$

But this is precisely the value that (17) assumes when sinh ΛD is replaced by ΛD, so that at large distances the results of Section (3) hold, ΛD being small. It is there shown that the results are valid provided that D/L is less than 0·2 so that the value D/L=1/5 represents the limit of application of the lamina theory for large distances.

9. *Limits of Lamina Theory at Small Distances.*

Confining ourselves to vertical points, divide (38) by (39). The correction factor for the lamina theory is then given by

$$1-\tfrac{1}{3}\gamma^2\beta+\tfrac{1}{3}j\gamma^2\,(G'+jG).$$

Assuming γ^2 small the correcting factor has amplitude

$$1-\tfrac{1}{3}\gamma^2\{\beta-G/(G'^2+G^2)\}.$$

Now $\gamma^2 = D\beta/y$ and the least value of y is $y=D$. In this case the correcting factor has amplitude

$$A = 1-\tfrac{1}{3}\beta\{\beta-G/(G^{12}+G^2)\},$$

from which we find

$\beta =$	0·2	0·4	0·6	0·8	1·0	2·0
A =	1·012	1·028	1·046	1·062	1·078	1·144
D/L =	0·071	0·101	0·123	0·142	0·159	0·225

Since the error has been over-estimated in (38) the above table shows that the lamina theory is less than 10 per cent. in error even for points on the surface when D/L is less than 1/6.

Field below the Surface of the Sea.

10. *Approximation for Moderate and Great Depths.*

The expression (9) for Δ may be simplified if the second term is negligible in comparison with the first. Now the second term has its largest relative value when $m = 0$, and then (9) becomes $\Delta = \Lambda^2\epsilon^{\Lambda D}(1 - \epsilon^{-2\Lambda D})$ in which $\epsilon^{-2\Lambda D}$ is the factor introduced by the second term. This term will have an effect of less than 1 per cent. if $\epsilon^{-2|\Lambda|D} < 0{\cdot}01$ so that from (3) we find that if D/L exceeds $0{\cdot}26$, the effect of the second term may be ignored if an accuracy of 1 per cent. is all that is required. With this approximation equations (15) become

$$\left.\begin{aligned} \mathrm{E}_1 &= 4j\omega\mathrm{I}_0\int_0^\infty \epsilon^{-m'y}\cos mx\, dm/(m+m') \\ \mathrm{E}_2 &= 4j\omega\mathrm{I}_0\int_0^\infty \epsilon^{-m'(2\mathrm{D}-y)}\cos mx\,(m'-m)\, dm/(m+m')^2 \end{aligned}\right\} \quad \ldots\ldots (48)$$

wherein a has also been put equal to zero so that the cable is now supposed to lie on the bed of the sea.

It will be seen that the depth D does not enter into the expression for E_1. In fact E_1 is the induced electric force at a height y above the cable when the depth of the sea is infinite. Also the way in which D occurs in E_2 indicates that E_2 may be regarded as arising from a source situated at the point $y = 2\mathrm{D}$ that is, at a height above the sea equal to the depth. Thus E_2 is the electric force representing a reflected disturbance due to the presence of the upper surface.

In order to study the forms of the integrals (48) it is convenient to transform them as follows :—

Put $m = \Lambda \sinh v$ so that $dm = \Lambda \cosh v\, dv$ and $m' = \Lambda \cosh v$.

Then

$$\left.\begin{aligned} \mathrm{E}_1 &= 2j\omega\mathrm{I}_0\int_0^\infty \epsilon^{-\Lambda y\cosh v}\cos(\Lambda x\sinh v)\,(1+\epsilon^{-2v})\, dv, \\ \mathrm{E}_2 &= 2j\omega\mathrm{I}_0\int_0^\infty \epsilon^{-\Lambda(2\mathrm{D}-y)\cosh v}\cos(\Lambda x\sinh v)\,(\epsilon^{-2v}+\epsilon^{-4v})\, dv, \end{aligned}\right\} \quad \ldots\ldots (49)$$

or using two sets of polar co-ordinates with the poles at

$y = 0$, $y = 2\mathrm{D}$, so that $y = \rho\cos\theta$, $2\mathrm{D} - y = \rho'\cos\theta'$, $x = \rho\sin\theta = \rho'\sin\theta'$,

$$\left.\begin{aligned} \mathrm{E}_1/2j\omega\mathrm{I}_0 &= \text{real part of } \int_0^\infty \epsilon^{-\Lambda\rho\cosh(v+i\theta)}(1+\epsilon^{-2v})\, dv, \\ \mathrm{E}_2/j\omega\mathrm{I}_0 &= \text{,,} \quad \text{,,} \quad \text{,,} \int_0^\infty \epsilon^{-\Lambda\rho'\cosh(v+i\theta')}(\epsilon^{-2v}+\epsilon^{-4v})\, dv. \end{aligned}\right\} \quad \ldots\ldots (50)$$

The integrals to consider are therefore all of the type

$$\mathrm{I}_n = \int_0^\infty \epsilon^{-\Lambda\rho\cosh(v+i\theta)}\epsilon^{-2nv}\, dv, \quad \ldots\ldots\ldots\ldots (51)$$

in which we are only concerned with the real part and n takes the values, 0, 1, 2.

To obtain the real part of (51) put

$$I_n = \epsilon^{2ni\theta}\int_{i\theta}^{\infty} \epsilon^{-\lambda\rho\cosh w}\,\epsilon^{-2nw}\,dw$$

$$= \epsilon^{2ni\theta}\left(i\int_{\theta}^{0}\epsilon^{-\lambda\rho\cos\theta}\cos 2n\theta\,d\theta + \int_{\theta}^{0}\epsilon^{-\lambda\rho\cos\theta}\sin 2n\theta\,d\theta + \int_{0}^{\infty}\epsilon^{-\lambda\rho\cosh w}\,\epsilon^{-2nw}\,dw,\right),$$

and the real part of I_n is

$$\cos 2n\theta\left(\int_{0}^{\infty}\epsilon^{-\lambda\rho\cosh w}\,\epsilon^{-2nw}\,dw - \int_{0}^{\theta}\epsilon^{-\lambda\rho\cos\theta}\sin 2n\theta\,d\theta\right)$$

$$+ \sin 2n\theta\int_{0}^{\infty}\epsilon^{-\lambda\rho\cos\theta}\cos 2n\theta\,d\theta \quad . \quad . \quad . \quad . \quad . \quad (52)$$

11. *Points Vertically over Cable.*

In the case $\theta = 0$ the real part of I_n in (52) becomes

$$\int_{0}^{\infty}\epsilon^{-\lambda\rho\cosh w}\,\epsilon^{-2nw}\,dw,$$

or upon substituting $u = w + j\pi/2$,

$$(-)^n\int_{0}^{\infty}\epsilon^{j\lambda\rho\sinh v}\,\epsilon^{-2nv}\,du,$$

a form of integral which may be expressed in Bessel functions and exponentials.

If this form is used in (49) (with $x = 0$) and the exponentials in u are converted to hyperbolic functions we obtain for E_1 and E_2

$$\left.\begin{aligned} E_1 &= 4j\omega I_0\int_{j\pi/2}^{\infty}\epsilon^{j\lambda\rho\sinh u}(1 - \cosh^2 u + \cosh u\sinh u)\,du \\ E_2 &= 4j\omega I_0\int_{j\pi/2}^{\infty}\epsilon^{j\lambda\rho\sinh u}\{1 - 5\cosh^2 u + 4\cosh^4 u \\ &\qquad - (4\sinh^2 u + 1)\cosh u\sinh u\}\,du \end{aligned}\right\} \quad (53)$$

Now the integral

$$\int_{j\pi/2}^{\infty}\epsilon^{t\sinh u}\cosh^{2n} u\,du$$

is converted to Bessel functions in GRAY and MATHEWS' 'Bessel Functions,' p. 61, the real part of t being negative, and the result is

$$(-)^n\frac{1\cdot 3\cdot 5\ldots 2n-1}{t^n}\left\{\left(\log 2 - \gamma + \frac{\pi}{2}j\right)J_n(t) - Y_n(t)\right\},$$

where Jn, Yn are Bessel functions of the first and second kind to argument t, and γ is EULER'S constant, viz.: $\gamma = 0{\cdot}57722$. The expression in $\{\ \}$ is that solution of

Bessel's equation which vanishes for large values of the argument, and therefore will be written $K_n(t)$. Using this result and solving the remaining integrals in (53) by elementary methods we get

$$\left.\begin{aligned}\frac{E_1}{4j\omega I_0} &= K_0(t) - \frac{K_1(t)}{t} + \left(\frac{1}{t^2} - \frac{j}{t}\right)\epsilon^{jt} \\ \frac{E_2}{4j\omega I_0} &= K_0(t') - \frac{5K_1(t')}{t'} + \frac{12K_2(t')}{t'^2} - \left(\frac{24}{t'^4} - \frac{24j}{t'^3} - \frac{11}{t'^2} + \frac{3j}{t'}\right)\epsilon^{jt'}\end{aligned}\right\} \quad \ldots (54)$$

in which using (3),

$$\left.\begin{aligned}t &= j\Lambda\rho = j\sqrt{j}\,2\sqrt{2}\pi\rho/L = j\sqrt{j}\xi \quad \text{say} \\ t' &= j\Lambda\rho' = j\sqrt{j}\,2\sqrt{2}\pi\rho'/L = j\sqrt{j}\xi'\end{aligned}\right\} \quad \ldots\ldots\ldots (55)$$

Equations (54) give the direct and reflected terms for the electric force at any point in the sea vertically above the cable in a form suitable for computation when tables of the appropriate Bessel functions are available. Now we have

$$\left.\begin{aligned}K_0(j\sqrt{j}\,\xi) &= ker\xi + j\,kei\xi) \\ K_1(j\sqrt{j}\,\xi) &= \sqrt{j}\,(ker'\xi + j\,kei'\xi) \\ K_2(t) &= \frac{2}{t}K_1(t) - K_0(t)\end{aligned}\right\}, \quad \ldots\ldots\ldots (56)$$

and tables of $ker\xi$, $kei\xi$, $ker'\xi$, $kei'\xi$ are given in 'British Assoc. Reports,' 1915, p. 36, so that there are sufficient numerical data available to regard (54) as the practical solution of the problem for points vertically over the cable. Corresponding formulæ for the *field* at points vertically above the cable may be obtained from (54) by differentiation using (1).

Computation Formulæ.—Using (56) to express K_2 in terms of K_1 and K_0 and differentiating to obtain the horizontal field we obtain the following formulæ for computing the electric force and field at points vertically over the cable.

$$\left.\begin{aligned}\frac{E_1}{4j\omega I_0} &= K_0(t) - \frac{K_1(t)}{t} + \left(\frac{1}{t^2} - \frac{j}{t}\right)\epsilon^{jt} \\ \frac{E_2}{4j\omega I_0} &= \left(1 - \frac{12}{t'^2}\right)K_0(t') + \left(\frac{24}{t'^3} - \frac{5}{t'}\right)K_1(t') - \left(\frac{24}{t'^4} - \frac{24j}{t'^3} - \frac{11}{t'^2} + \frac{3j}{t'}\right)\epsilon^{jt'} \\ \frac{P_1}{4j\Lambda I_0} &= \frac{K_0(t)}{t} - \left(1 - \frac{2}{t^2}\right)K_1(t) + \left(\frac{2}{t^3} - \frac{2j}{t^2} - \frac{1}{t}\right)\epsilon^{jt} \\ \frac{P_2}{4j\Lambda I_0} &= \left(\frac{48}{t'^3} - \frac{5}{t'}\right)K_0(t') - \left(\frac{96}{t'^4} - \frac{22}{t'^2} + 1\right)K_1(t') \\ &\quad + \left(\frac{96}{t'^5} - \frac{96j}{t'^4} - \frac{46}{t'^3} + \frac{14j}{t'^2} + \frac{3}{t'}\right)\epsilon^{jt'}\end{aligned}\right\} \quad \ldots\ldots (57)$$

In these formulæ t, t' are as defined in (55), Λ is defined in (3), the whole electric force is given by $E = E_1 + E_2$, and the whole field by $P = P_1 + P_2$.

Table VIII. has been computed from equations (57).

12. *Current Density Vertically over Cable.*

The current density at a point at a height ρ above the cable is given by

$$i = kE = 4j\omega k I_0 \, (E_1/4j\omega I_0 + E_2/4j\omega I_0),$$

$$= j \frac{\xi^2 I_0}{\pi\rho^2} \, (E_1/4j\omega I_0 + E_2/4j\omega I_0),$$

since $4\omega k = \xi^2/\pi\rho^2$ by (55) and (3).

Thus $\rho^2 i/I_0$ is a function of ξ, ξ' only, and may be calculated with the help of Table VIII. By calculating a series of values the Charts 5 and 6 have been constructed.

Both charts are plotted with $\xi_{max} \equiv 2\sqrt{2}\,\pi D/L$ as abscissæ and ρ/D as ordinates.

Chart 5 gives the lines $\rho^2 |i|/I_0 =$ constant where $|i|$ is the *amplitude* of i and Chart 6 gives the lines of constant phase of current density. The results of Table VIII may not be used when ξ_{max} is less than 2·5 because of the restriction imposed in Section 10.

However, by making use of the results of the lamina theory we can obtain the starting points of the lines at the top surface when ξ_{max} is less than 1·8. Starting from these points the unknown region may be filled in at any rate approximately using the general directions of the known lines as a guide.

13. *Horizontal Field vertically over Cable.*

If P_0 is the undisturbed field so that $P_0 = 2I_0/\rho$ then

$$\frac{P}{P_0} = j\sqrt{j}\,\xi \left(\frac{P_1}{4j\Lambda I_0} + \frac{P_2}{4j\Lambda I_0} \right),$$

so that P/P_0 is a function of ξ, ξ'.

The variation of P/P_0 with vertical height is too rapid to permit of immediate graphical representation, so that the following procedure has been adopted.

If the variation were that of a plane wave then ($|P|$ being the amplitude of P) $|P|/P_0$ would vary as $\epsilon^{-2\pi\rho/L}$ or $|P|\epsilon^{2\pi\rho/L}/P_0$ would be constant. In the actual case this is not so, but we write

$$F = |P|\epsilon^{2\pi\rho/L}/P_0.$$

F is a quantity varying only slowly and is suitable for plotting. The lines F = constant are plotted on Chart 7. Finally Chart 8 gives the lines of constant phase for the magnetic field (Plate 4).

In regard to the region for which ξ_{max} is less than 2·5 the remarks of the last section hold.

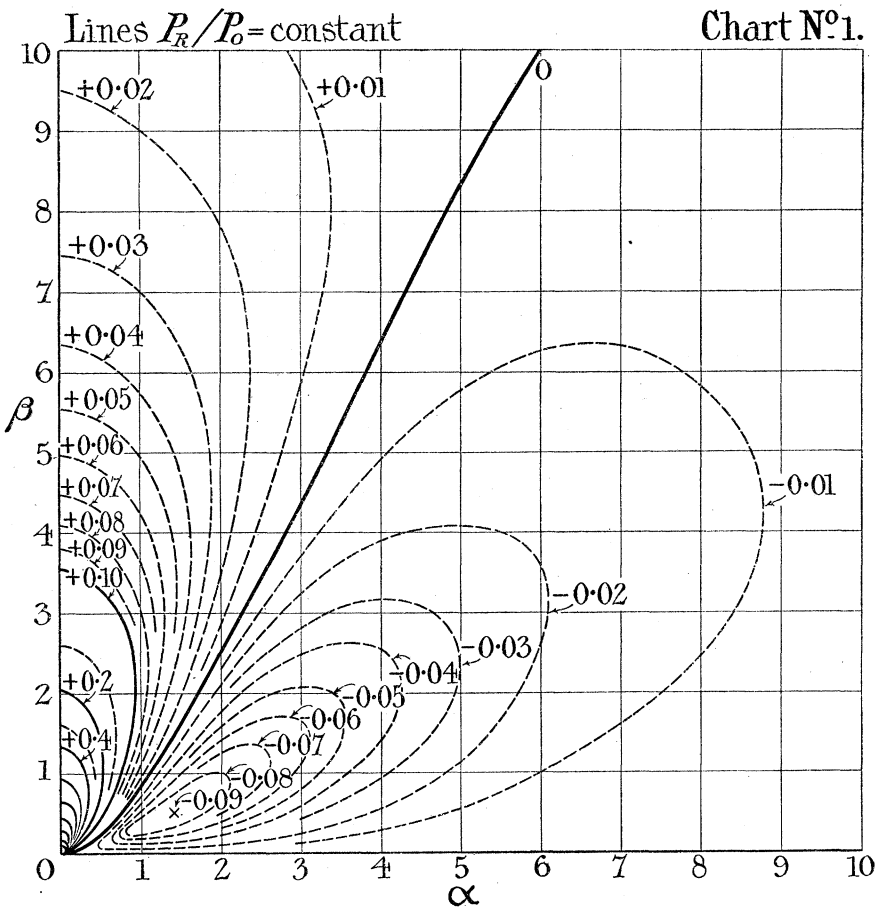

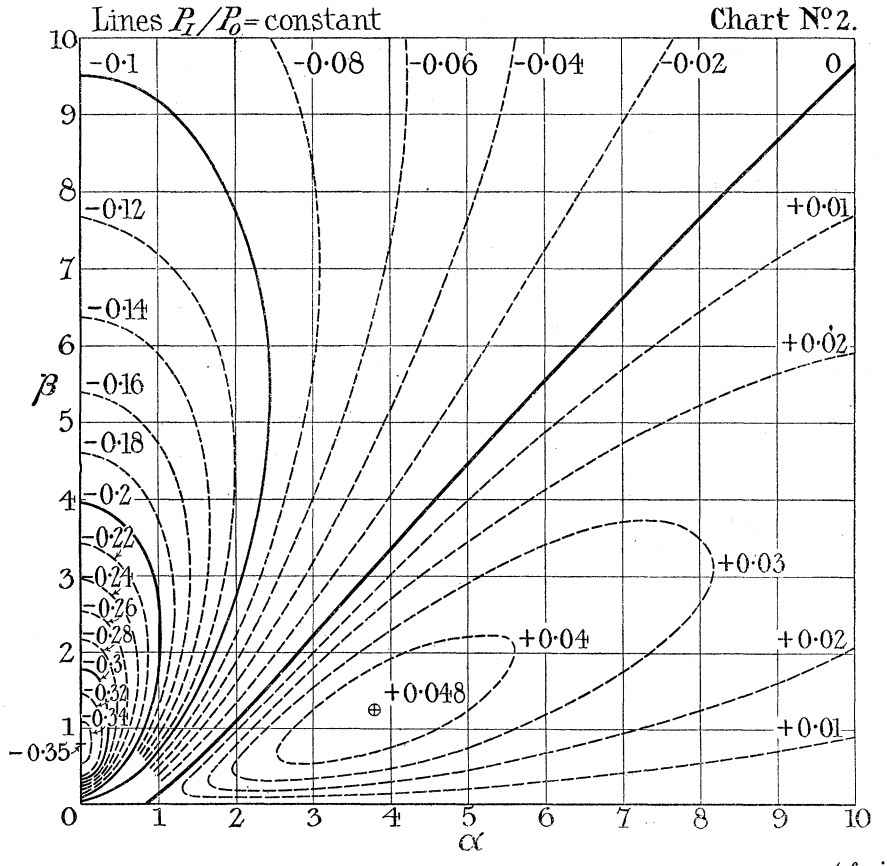

(*facing p.* 154.)

PHILOSOPHICAL TRANSACTIONS OF THE ROYAL SOCIETY A MATHEMATICAL, PHYSICAL & ENGINEERING SCIENCES

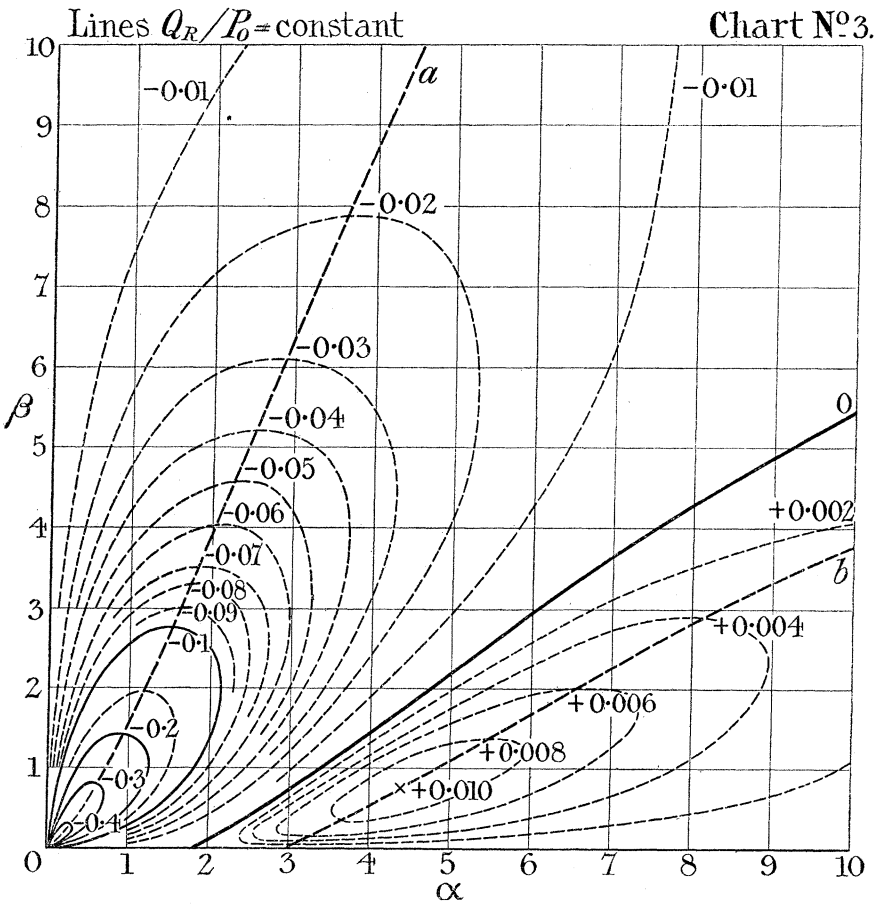

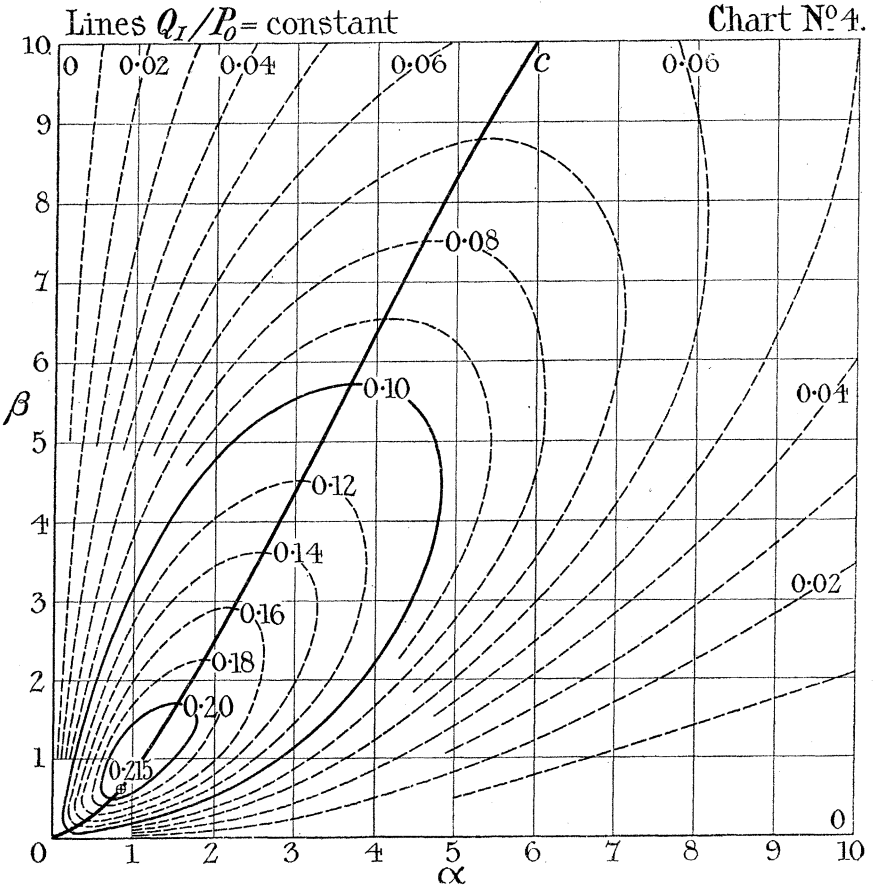

PHILOSOPHICAL TRANSACTIONS OF THE ROYAL SOCIETY A MATHEMATICAL, PHYSICAL & ENGINEERING SCIENCES

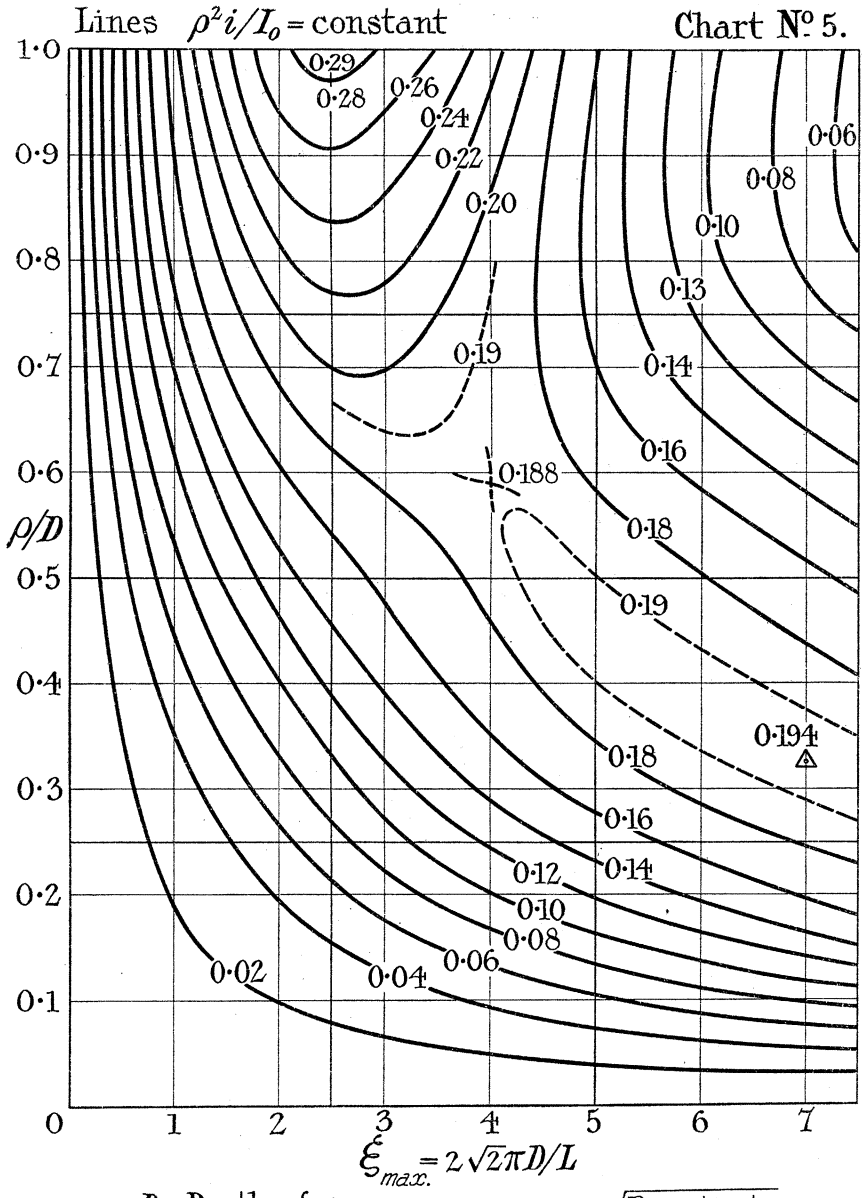

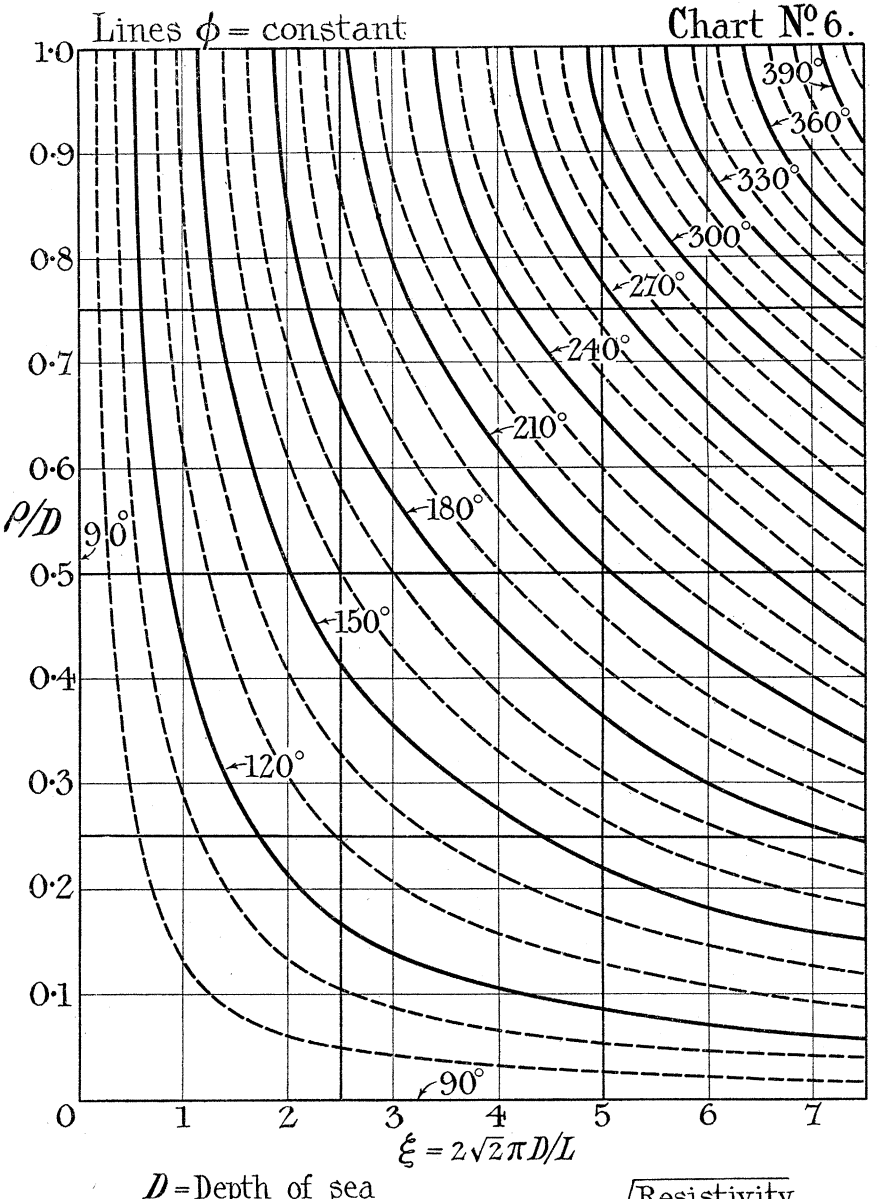

Butterworth. Phil. Trans., A, vol. 224, Plate 3.

PHILOSOPHICAL TRANSACTIONS OF THE ROYAL SOCIETY A MATHEMATICAL, PHYSICAL & ENGINEERING SCIENCES

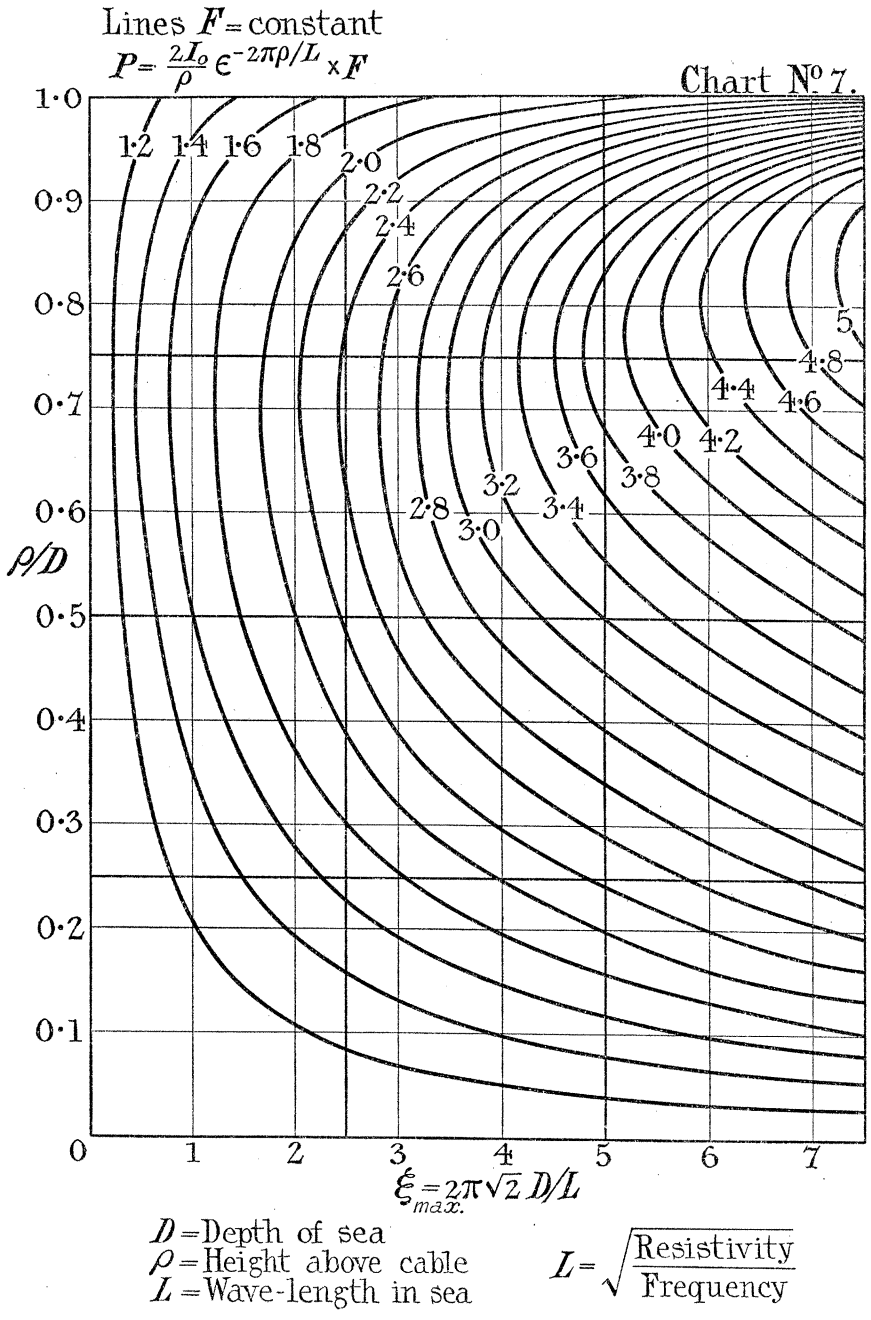

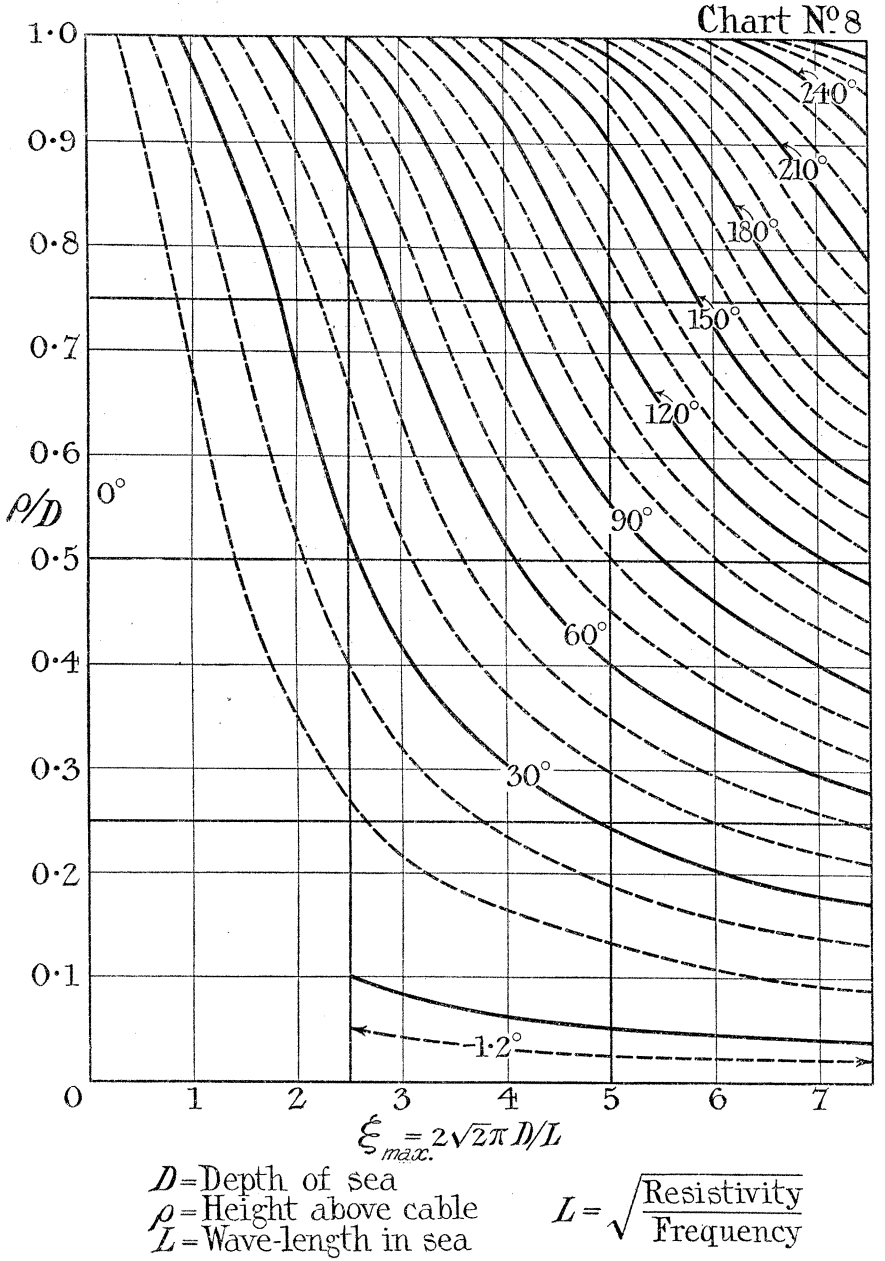

Butterworth. Phil. Trans., A, vol. 224, Plate 4.

14. *Points at Large Distances from the Cable.*

Returning to the results obtained in Section 10, we require the form of the expression (52) when ρ is very large and θ is nearly 90 degrees. The first integral which has been considered in section 11 vanishes when $\Lambda\rho$ is very large in the same way as $\epsilon^{-\Lambda\rho}/\sqrt{\rho}$, while the remaining integrals which only contain ρ in association with $\cos\theta$ do not vanish so quickly because $\rho\cos\theta = y$ does not vary with increase of x. We need therefore only the two latter integrals and in these integrals we can assume θ is nearly 90 degrees not only outside the signs of integration, but also inside, because since ρ is large the integrand is negligible except in the immediate neighbourhood of the upper limit. Putting therefore $\theta = \frac{\pi}{2} - \phi$ and assuming ϕ small, we have from (52)

$$\text{Real part of } \mathrm{I}_n = 2n\left\{\int_{\phi}^{\frac{\pi}{2}} \phi\epsilon^{-\Lambda\rho\phi}\,d\phi - \phi\int_{\phi}^{\frac{\pi}{2}} \epsilon^{-\Lambda\rho\phi}\,d\phi\right\}$$
$$= 2n\epsilon^{-\Lambda\rho\phi}/\Lambda^2\rho^2$$

again neglecting the upper limit term because of the large value of $\Lambda\rho$. Also to the same approximation

$$\rho\phi = \rho\cos\theta = y$$

and

$$\text{Real part } \mathrm{I}_n = 2n\epsilon^{-\Lambda y}/\Lambda^2\rho^2.$$

Further from (50)

$$\left.\begin{aligned}\mathrm{E}_1/2j\omega\mathrm{I}_0 &= 2\epsilon^{-\Lambda y}/\Lambda^2\rho^2\\ \mathrm{E}_2/2j\omega\mathrm{I}_0 &= 6\epsilon^{-\Lambda y'}/\Lambda^2\rho'^2\end{aligned}\right\}. \qquad (58)$$

For these large distances ρ, ρ' may be considered equal and may be identified with the horizontal distance x.

The total electric force E is obtained by adding E_1 and E_2 so that

$$\mathrm{E} = \frac{4j\omega\mathrm{I}_0}{\Lambda^2x^2}\{\epsilon^{-\Lambda y} + 3\epsilon^{-\Lambda(2\mathrm{D}-y)}\}, \qquad (59)$$

since

$$y' = 2\mathrm{D} - y.$$

Expressed in terms of depth d below the upper surface,

$$d = \mathrm{D} - y$$

and

$$\mathrm{E} = \frac{8j\omega\mathrm{I}_0}{\Lambda^2x^2}\epsilon^{-\Lambda\mathrm{D}}(2\cosh\Lambda d - \sinh\Lambda d). \qquad (60)$$

By differentiation the corresponding expression for the horizontal field is

$$\mathrm{P} = \frac{8\mathrm{I}_0}{\Lambda x^2}\epsilon^{-\Lambda\mathrm{D}}(2\sinh\Lambda d - \cosh\Lambda d). \qquad (61)$$

The vertical field is proportional to $\partial E/\partial x$ and therefore to $1/x^3$, so that at large lateral distances the field becomes more and more nearly horizontal, instead of vertical as would be the case if the sea had no conductivity.

At the *upper* surface $d = 0$ and

$$E = 16 j\omega I_0 \epsilon^{-\Lambda D}/\Lambda^2 x^2, \qquad P = -8 I_0 \epsilon^{-\Lambda D}/\Lambda x^2. \quad (62)$$

From the last result using the value of Λ as given by (3) $|P|$ the amplitude of P is given by

$$|P| = \frac{2\sqrt{2}}{\pi} \frac{I_0 L}{x^2} \epsilon^{-2\pi D/L}. \quad (63)$$

The result (62) is identical with equation (21), which was arrived at from considerations of the field above the surface of the sea. At the *lower* surface $d = D$ and since $\epsilon^{2\pi D/L}$ is small

$$E = 4 j\omega I_0/\Lambda^2 x^2, \qquad P = 4 I_0/\Lambda x^2 \quad (64)$$

giving

$$|P| = \sqrt{2} I_0 L/\pi x^2. \quad (65)$$

The field at the bed of the sea is thus much stronger than that at the surface, a result which may be of considerable practical importance.

15. *Distant Field regarded as due to Two Plane-Waves.*

The disturbances at large lateral distances may be considered as made up of two plane-waves travelling at right angles to the bounding surface. The wave directed upwards is specified by E_1 in (58) and starts at the bed of the sea with a value $E_1 = 4 j\omega I_0/\Lambda^2 x^2$ while the wave E_2 travels downwards having the initial value $E_2 = 12 j\omega I_0 \epsilon^{-\Lambda D}/\Lambda^2 x^2$. It is useful to consider these waves from the point of view of energy flow. The wave E_1 pours energy into the sea from the bed and the wave E_2 introduces energy from above. Moreover, although E_1 is initially much greater than E_2, the wave E_2 predominates in the neighbourhood of the upper surface. There is therefore a comparatively narrow region at the upper surface of the sea which is being supplied with electromagnetic energy from the upper air while the bulk of sea below is obtaining the energy to produce its eddy currents from the region below the sea. The plane dividing these two regions may be determined by a simple application of POYNTING's theorem, which asserts that the instantaneous energy flow per second per sq. cm. is given by $ep/4\pi$, where e and p are the instantaneous values of E and P. In general the energy flow may be analysed into an alternating flow and a steady flow, the relative values of the two flows being governed by the relative phases of E and P. In particular the steady flow is zero when E and P are in quadrature. As we pass through the plane for which E and P are in quadrature the direction of the steady flow reverses, so that to find the plane separating the regions specified above we require the depth at which the phase

difference between E and P becomes 90 degrees. Analytically by (60) and (61) we require the condition that

$$\frac{j}{\Lambda}\,\frac{2\cosh \Lambda d - \sinh \Lambda d}{2\sinh \Lambda d - \cosh \Lambda d}$$

shall be purely imaginary.

Putting $\Lambda d = \eta\,(1+j)$, in which $\eta = 2\pi d/\mathrm{L}$, and equating the real part of the above expression to zero, the condition becomes

$$4\sinh 2\eta - 4\cosh 2\eta + 3\sin 2\eta = 0 \quad \ldots\ldots\ldots\ldots (66)$$

giving, by trial and error,

$$\eta = 0{\cdot}2885\,;$$

so that the depth d required is

$$d = 0{\cdot}0459\ \mathrm{L}.$$

For example, if the resistivity of sea water is 25 ohms per c.c. and the frequency of the electro-magnetic waves is 500 ~ per second, $\mathrm{L} = \sqrt{\rho/f} = 70{\cdot}7$ metres, $d = 3{\cdot}25$ metres.

Thus the eddy currents in the first 3·25 metres of the sea are produced by energy derived from the upper air, while the eddy currents in the remaining portions of the sea derive their energy from below.

16. *Variation of Field and Current Density with Depth.*

The following results have been derived from equations (60) and (61) using KENNELLY'S tables of complex hyperbolic functions. The current density $|i|$ and magnetic field $|\mathrm{P}|$ are expressed as fractions of their upper surface value. The depth d is represented by $\xi = 2\sqrt{2}\pi d/\mathrm{L}$, from which the true depth can be found when the wave-length is known.

ξ.	Current Density.		Field.	
	$\lvert i\rvert$	Lag behind Surface Value.	$\lvert \mathrm{P}\rvert$	Lag behind Surface Value.
		°		°
0	1·000	0	1·000	0
0·2	0·933	+ 4·1	0·772	+ 21·2
0·4	0·864	+ 4·3	0·671	+ 48·1
0·6	0·788	+ 3·2	0·734	+ 74·5
0·8	0·732	− 0·7	0·926	+ 91·4
1·0	0·672	− 7·6	1·159	+100·4
1·2	0·630	−18·2	1·402	+104·4
1·4	0·624	−31·9	1·640	+104·25
1·6	0·648	−48·0	1·898	+103·9
1·8	0·728	−63·6	2·15	+100·6
2·0	0·856	−77·3	2·40	+ 96·3
2·2	1·023	−87·5		
2·4	1·235	−98·9		

It is seen from the table that as we proceed downwards from the surface both current density and field first diminish in value and afterwards rise, while the phase lag first increases and then diminishes. As regards the variations in amplitude, the surface value of the field will be exceeded as depths greater than 0·097 of a wave-length and the surface value of the current density will be exceeded when the depth is greater than 0·244 of a wave-length. At a frequency of 500 per second the wave-length is 70·7 metres if the sea has a resistivity of 25 ohms per c.c., so that the depths to be used in order to obtain more sensitive reception than at the surface must exceed 6·8 metres when receiving by field and 17·2 metres when receiving by current density.

II. Experimental.

Study of Field Distribution above the Surface of the Sea by means of a Lead Model.

1. *Principle of Model.*

If a long straight cable carrying alternating current is covered by a large non-magnetic conducting sheet then, if we confine ourselves to distances which are small compared with the wave-length of electromagnetic propagation either along the cable or in the air, the reduction of field at any point due to the eddy currents induced in the sheet depends only on the frequency (f) of the current, the conductivity (k) of the sheet and its depth (D) which is assumed uniform.

Thus if R be the reduction factor

$$\mathrm{R} = \mathrm{F}(k, f, \mathrm{D}) \quad . \quad . \quad . \quad . \quad . \quad . \quad . \quad . \quad . \quad . \quad . \quad . \quad (1)$$

Since R is non-dimensional every member of the right-hand side of (1) must also be non-dimensional. This can only be so if k, f, D are always associated in the form $kf\mathrm{D}^2$.

Therefore at a fixed point $\mathrm{R} = \mathrm{F}(kf\mathrm{D}^2)$ or putting $\mathrm{L}^2 = 1/kf$ so that L is a length depending only on the material and frequency

$$\mathrm{R} = \mathrm{F}(\mathrm{D}/\mathrm{L}) \quad . \quad . \quad . \quad . \quad . \quad . \quad . \quad . \quad . \quad . \quad . \quad . \quad (2)$$

Extending to all points and remembering that the field will not vary along lines parallel to the cable

$$\mathrm{R} = \mathrm{F}\left(\frac{x}{\mathrm{L}}, \frac{y}{\mathrm{L}}, \frac{\mathrm{D}}{\mathrm{L}}\right), \quad . \quad . \quad . \quad . \quad . \quad . \quad . \quad . \quad . \quad . \quad . \quad . \quad (3)$$

where x, y are co-ordinates in a plane perpendicular to the cable.

Thus a reduction factor determined at a given point using one material may be applied to a corresponding point using another material provided that x/L, y/L, and D/L are the same for both materials.

This principle may be used to construct a model for studying on a small scale the distribution of magnetic field above the surface of the sea due to a submarine cable carrying alternating currents.

All that is required is that the ratio of the characteristic length L for the material chosen to the thickness of the material shall be the same as that for the sea. Since L^2 is proportional to the resistivity of the material at a given frequency a model for which 1 millimetre will represent 1 metre may be constructed if we choose a material whose conductivity is one million times that of sea-water, and as lead is suitable for other reasons the following experiments were carried out, using lead to represent the sea.

It may be noted that the characteristic length L is the wave-length of plane damped electro-magnetic waves propagated at frequency f through an infinite medium of conductivity k.

2. *Quantities to be measured.*

The field at any point in the air above the cable is determined by four quantities, viz.: the amplitude and phase with respect to the cable current of the field components parallel and perpendicular to the sheet. Actually it was found more convenient to measure the in-phase and quadrature components of the horizontal and vertical field. Denoting the former four quantities by P, ϕ_P, Q, ϕ_Q, and the latter four by P_R, P_I, Q_R, Q_I, we have

$$\left.\begin{aligned} P_R &= P\cos\phi_P, & Q_R &= Q\cos\phi_Q \\ P_I &= P\sin\phi_P, & Q_I &= Q\sin\phi_Q \end{aligned}\right\} \quad \ldots\ldots\ldots (4)$$

In expressing the results sometimes one and sometimes the other system is used according to convenience.

3. *Method of Measurement.*

A search coil placed in the alternating field above the sheet will have induced in it an electromotive force proportional to the current in the cable and bearing a definite phase relation to the current. If in the search coil circuit we induce an equal and opposite electromotive force from the same source there will then be no action on a detecting instrument included in the circuit and the balance will be independent of fluctuations in the source. The known value of the latter electromotive force gives the induced electromotive force in the search coil, and the mean field normal to the plane of the search-coil follows from the formulæ

$$E = \omega HA \quad \ldots\ldots\ldots\ldots\ldots\ldots (5)$$

in which E is the measured electromotive force, $\omega/2\pi$ the frequency, A the effective area of the coil, and H the field required. The phase of the field is 90° ahead of the electromotive force. The field so measured will include stray fields and may be in error

due to capacity currents flowing through the search coil circuits. Both these errors should be eliminated by using the following method.

With the search coil in the circuit but with the cable not in, let two balanced electromotive forces be impressed on the search coil circuit. Let current flow through the cable and readjust one of the electromotive forces for a new balance. Then the change required gives the electromotive force due to the introduction of the cable field into the search coil.

This method was realised in the manner shown in fig. 2. When the switch is at the

Fig. 2.

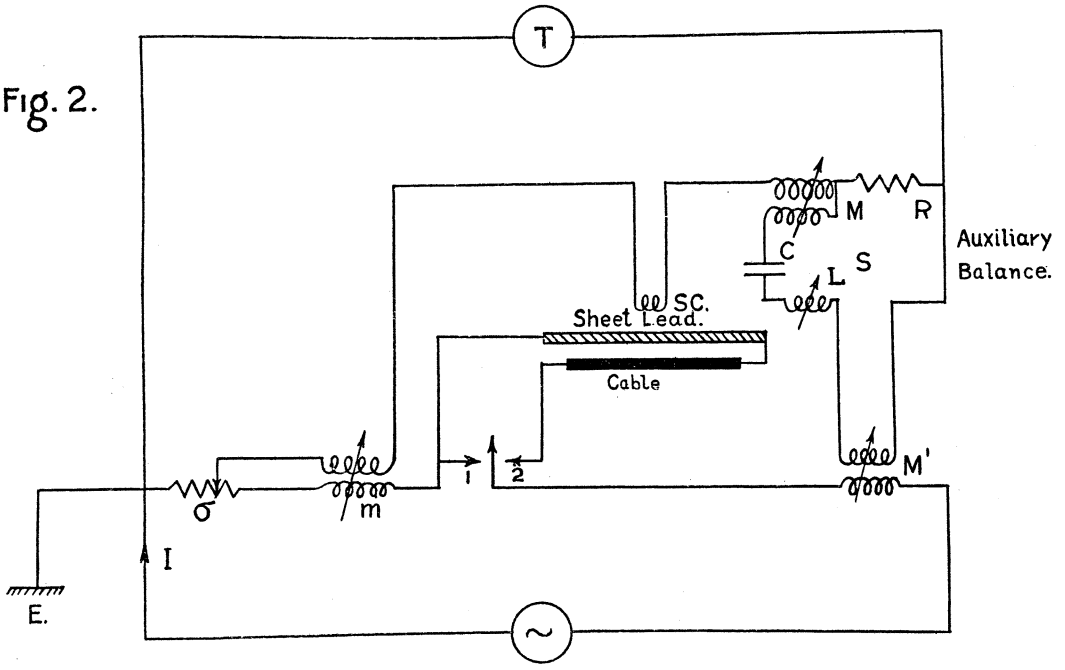

point 2, the main circuit acts on the telephone circuit through three couplings :—

(1) from cable to search coil giving electromotive force E ;

(2) through the adjustable slide wire σ and mutual inductance m giving electromotive force

$$E_1 = (\sigma + j\omega m)\, I ;$$

(3) through the resonating circuit L C of total resistance S, which is coupled to the main circuit by the mutual inductance M′ and to the telephone circuit by the pair M, R. This system impresses an electromotive force

$$E_2 = \frac{j\omega M'}{S}(R + j\omega M)$$

on the telephone circuit when $\omega^2 L C = 1$.

The resonance condition is not essential as E_2 is merely required to give an auxiliary balance. It is, however, convenient in predetermining the value of E_2 to balance E_1.

The condition may rapidly be secured by making $\sigma = 0$, $M = 0$, and adjusting R and L for balance.

The system is earthed at the point shown in order to keep the telephone circuit at earth potential, and thus to eliminate troubles due to capacity currents between the telephone and the head of the observer.

In making a measurement σ, m are placed at convenient values and with the switch at 1, E_2 is adjusted for balance. The cable current is then switched on and σ, m are readjusted for balance to the new values σ', m'.

We then have

$$E = \{\sigma - \sigma' + j\omega\,(m - m')I\} \quad . . . . . (6)$$

so that by (5) if H_R, H_I represent the in-phase and quadrature components of the field to be measured

$$H_R = (m' - m)\,I/A, \qquad H_I = (\sigma - \sigma')\,I/\omega A. \quad . . . . . (7)$$

4. *Details of Apparatus.*

The cable was represented by 2·5 metres of No. 27 D.C.C. wire over which was placed a large sheet of lead of area 225 cm. × 119 cm. and 0·39 cm. thick in the region of measurement. The wire was parallel to the long edges and at a distance of 25 cm. from one of them. At corresponding frequencies this sheet thus represented a rectangular sheet of water 2250 metres by 1190 metres and 4 metres deep, having a submarine cable 250 metres from the shore. The cable was purposely placed out of centre in order to examine shore effect. This, however, turned out to be practically negligible. By employing higher frequencies on the model, greater depths and correspondingly greater areas could be represented. After all observations had been taken on the thin sheet a strip 200 cm. × 45 cm. × 0·76 cm. was added symmetrically over the table, and subsequently a third strip of the same area and 0·73 cm. thick was superposed.

Thus the three depths represented were 4 metres, 11·5 metres, 18·8 metres, and intermediate and greater depths could be represented by the principle of corresponding frequencies.

The resistivity of the lead was obtained by sample measurements and had an average value of 22·1 microhms per cm. cube.

The search coils were such that each turn embraced a long rectangle whose mean width was equal to the winding length. Two were used, a small coil having overall dimensions 20 cm. × 2 cm. × 2 cm. and a turn area of 13,700 sq. cm., and a large coil 20 cm. × 3·5 cm. × 3·5 cm. with a turn area of 100,000 sq. cm. The large coil was used for the measurement of the very weak fields at distant points. In all measurements the long side of the coil was parallel to the cable and the coil could be made to measure either horizontal or vertical field by rotation through a right angle.

It is essential that the mean field measured shall refer to a square area perpendicular to the cable as in this case the mean field is most nearly equal to the central field.

The resistance σ consisted of a manganin strip wound round the cylindrical surface of an ebonite disc, the current returning by practically the same path through a similar strip interposed between the outer strip and the disc. This arrangement made the system non-inductive. The resistance was varied by a rotating contact, the arm carrying the contact also carrying a pointer moving over a circular scale calibrated to read the resistance which varied from 0·01 to 0·14 ohm. The measured inductance of this resistance was less than 0·03 microhenry.

The mutual inductance m had a range of 10 microhenries and was subdivided to 0·1 microhenry. Readings could be taken to 0·02 microhenry. The alternating current was obtained from a valve source and gave a primary current of approximately 0·1 ampere. Four frequencies were used, viz. :—

596, 950, 1230, and 1870 cycles per second.

The system E_2 need not be described as its function is merely to supply an auxiliary balance.

5. *Range of Tests.*

The highest value of D/L for which measurements were taken was D/L = 0·443, using a thickness of lead of 1·88 cm. and a frequency of 1230 cycles. In the case of sea-water of resistivity 25 ohms per cm. cable at a frequency of 500 this corresponds to a depth of 31·3 metres or 17 fathoms, and to greater depths for lower frequencies.

The lowest plane which it was possible to explore with the coils used was at a height above the surface equal to about half the depth of the lead.

6. *Consistency Tests.*

Preliminary observations were made with various positions of the source, reversing both source and telephone connections as well as the circuit inductances. With the small coil, these revealed no inconsistency, but with the large coil a different value of E was obtained when the coil was rotated through 180° although the method cancels out the effect of stray flux through the search coil in each position. The effect was attributed to a capacity current flowing from the search coil to the sheet which altered its path and presumably its value as the switch was thrown over from position 1 to position 2. In fact a condenser connected from search coil to sheet increased the discrepancy. Since this capacity current produces an effect in the same direction when the coil is rotated through 180°, while the field due to the cable is reversed, the difference between the results in the two positions should separate out an effect of this kind. This was found to be the case when an artificial capacity effect was introduced, so the procedure was adopted in all readings with the large coil.

7. *Results with Thin Sheet.*

Using $\rho = 22{\cdot}1$ microhms per cm. cube, D = 0·385 the values of D/L for a frequency of 1870 $\sim$ per second is 0·112, so that the results all fall within the scope of the lamina

theory. For points vertically over the cable the reduction factor P/P_0 (P_0 being the undisturbed field $2I/H$) and the phase angle ϕ_P should be functions of $\beta = 4\pi^2 DH/L^2$ where H is the height above the cable. The theoretical values of P/P_0 and ϕ_P are given in Table II. All the results obtained for values of $\beta < 10$ are plotted in fig. 3, the full

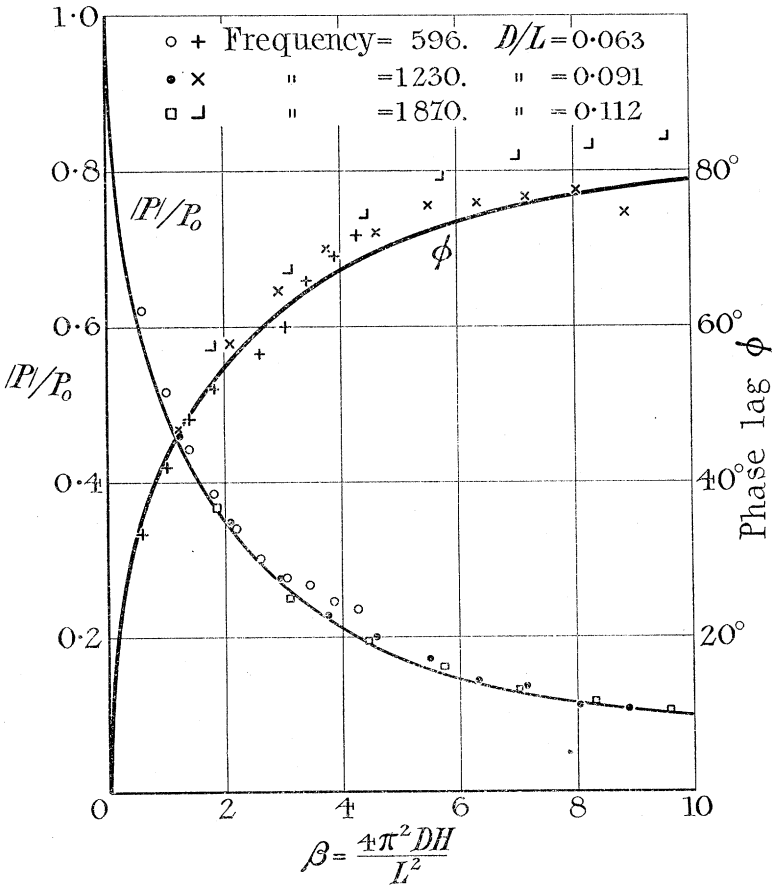

Fig. 3. Magnetic field vertically over cable. Small values of D/L.
Full curves represent theoretical values.
$|P|$ = Observed field. P_0 = Undisturbed field.

curves being the values predicted by the lamina theory. The agreement in regard to amplitude is very marked, but the observed phase angles are on the whole distinctly higher than the theoretical phase. Apart from the fact that the departure of the lamina theory from the truth is initially one of phase rather than of amplitude it must be remembered that the effect of the finite width of the sheet becomes more pronounced as the height increases. The effect is accounted for by a small diminution of the in-phase component of the field due to the finite width of the return current path.

For values of β greater than 10, the lamina theory gives the simple result,

$$P/P_0 = 1/\beta.$$

The following table indicates how nearly this result is verified :—

Frequency = 1230.				Frequency = 1870.			
H cm.	β.	P/P_0.		H cm.	β.	P/P_0.	
		Observed.	$1/\beta$.			Observed.	$1/\beta$.
10·2	8·7	0·112	0·115	7·45	9·6	0·104	0·104
13·2	11·2	0·087	0·089	8·45	10·9	0·092	0·092
16·2	13·8	0·075	0·072	9·2	11·9	0·087	0·084
19·2	16·3	0·059	0·061	9·45	13·5	0·078	0·074
22·2	18·9	0·053	0·053	11·2	14·4	0·069	0·069
				13·2	17·0	0·055	0·059

For points not vertically over the cable the theoretical values are obtained from the contour diagrams shown in Charts 1, 2, 3 and 4 (Plates 1 and 2).

As a typical traverse we take the case $f = 1230$, and $H = 1{\cdot}5$ cm., which corresponds to $\beta = 1{\cdot}28$. The values of P_R/P_0, P_I/P_0 are plotted in fig. 4 against $\alpha = 4\pi^2 Dx/L^2$,

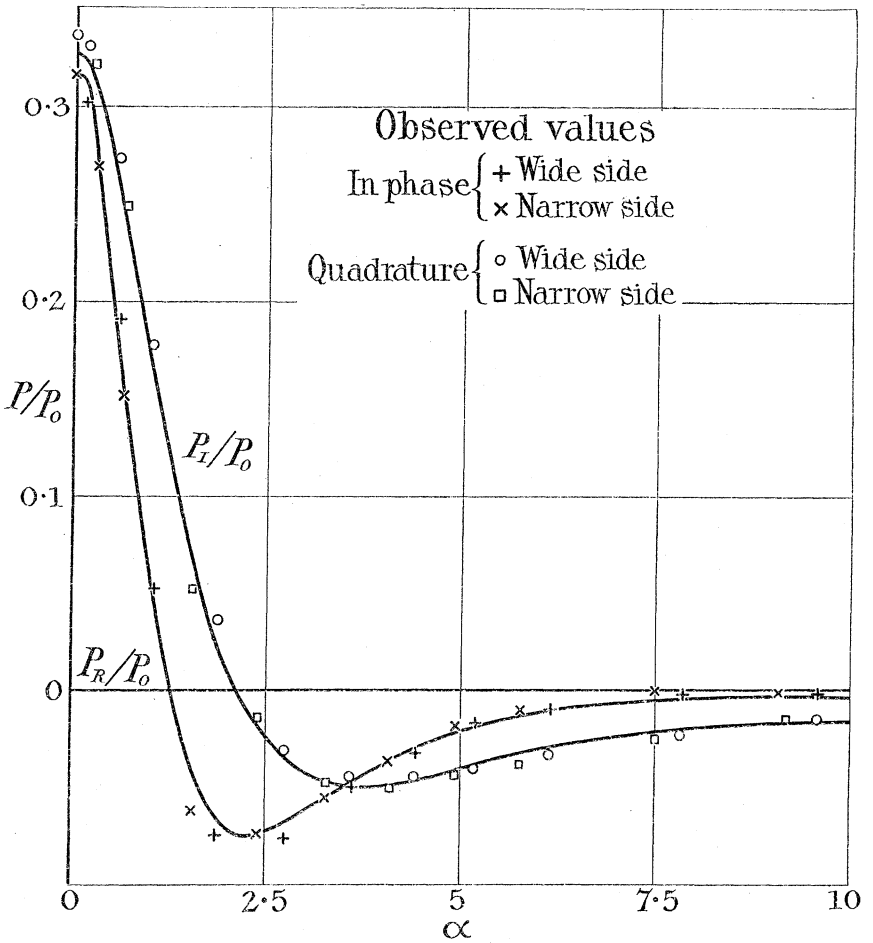

Fig. 4. Curves give theoretical values.
Horizontal field $\sim$ = 1230. Thickness of lead = $0{\cdot}38_5$ cm.
Mean height of search coil 1·4 cm. above cable.

x being the horizontal distance from the cable. The values of Q_R/P_0 and Q_I/P_0 are plotted against α in fig. 5. The full curves give the theoretical values and the observed points are marked in. The agreement of theory and practice is again very close, and the symmetry is good on either side the cable.

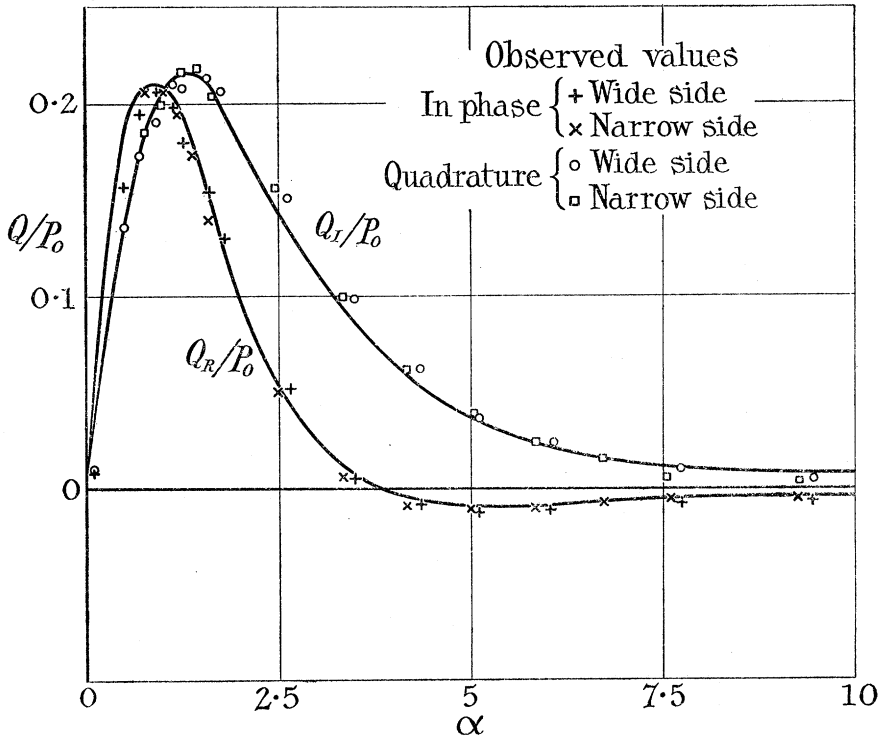

Fig. 5. Curves give theoretical values.
Vertical field $\sim$ = 1230. Thickness of lead = $0{\cdot}38_5$ cm.
Mean height of search coil = 1·55 cm. above cable.

For the purpose of comparing other traverses with theory the positions and values of the various maxima and the positions of the zeroes may be used. Theory gives the following sequence as we pass out from the vertical :—

(1) Q_R is maximum.
(2) Q_I is maximum and P_R is zero at the same point.
(3) P_R has a secondary maximum and immediately afterwards (if $\beta > 1$) P_I is zero.
(4) Q_R is zero and P_I has a secondary maximum at the same point.
(5) Q_R has a secondary maximum.

For large values of β these properties occur when the angular distances from the vertical are

22·5°, 30°, 45°, 60°, 67·5° respectively.

The properties were tested for five traverses as follows :—

Traverse.	A.	B.	C.	D.	E.
Frequency	596	1230	1870	1230	1230
H cm.	2·50	1·50	1·50	4·0	10·0
β	1·03	1·28	1·90	3·4	8·5

The following results were obtained :—

TRAVERSES over Thin Sheet. Position of Various Maxima and Zeroes.

β.	Q_R Max.		Q_R max.	P_R zero.		P_R sec. max.	P_I zero.		Q_R zero.	P_I sec. max.		Q_R sec. max.	
	Obsd.	Theory.	Observed.		Theory.	Observed.		Theory.	Observed.		Theory.	Obsd.	Theory.
1·03	0·8 0·8	0·75	1·2 1·0	1·0 1·1	1·08	1·9 2·0	2·1 1·9	1·90	3·7 3·5	4·5 4·5	3·4	—	4·95
1·28	0·9 1·0	0·88	1·30 1·35	1·15 1·2	1·24	2·0 2·4	2·1 2·2	2·14	3·6 3·7	4·0 3·8	3·8	5·5 5	5·35
1·90	1·2 1·2	1·15	1·95 1·85	1·5 1·55	1·65	2·5 2·9	2·7 2·8	2·70	4·2 4·1	5 5	4·2	6·3 6	6·3
3·4	2·0 1·8	1·8	2·8 2·8	2·4 2·4	2·52	4·2 5	3·8 4	4·05	8·6 5·6	8·5 7	6·8	— 7·5	9·2
8·5	3·6 4	3·9	5·3 5·3	4·7 4·7	5·12	8 8·4	8·6 8·9	8·85	14 11	15 15	15	14 14	20

The tabulated numbers give the value of α at which the particular property occurs, the upper number always referring to the narrow side of the sheet.

VALUES of Various Maxima.

β.	Q_R/P_0.		Q_I/P_0.		P_R/P_0 (sec.).		P_I/P_0 (sec.).		Q_R/P_0 (sec.).	
	Observed.	Theory.	Observed.	Theory.	Observed.	Theory.	Observed.	Theory.	Observed.	Theory.
1·03	0·275 0·250	0·248	0·212 0·216	0·206	0·084 0·090	0·080	0·054 0·040	0·046	—	0·009
1·28	0·206 0·206	0·210	0·216 0·214	0·215	0·076 0·079	0·074	0·052 0·046	0·050	0·010 0·012	0·009
1·90	0·140 0·135	0·155	0·190 0·195	0·194	0·062 0·062	0·056	0·048 0·046	0·044	0·015 0·015	0·008
3·4	0·065 0·056	0·076	0·143 0·145	0·145	0·028 0·029	0·026	0·040 0·040	0·032	— 0·008	0·002
8·5	0·013 0·0135	0·019	0·077 0·070	0·072	0·005 0·008	0·007	0·016 0·016	0·015	— 0·002	0·001

8. *Results with Thicker Sheets.*

(A) *Points vertically over the Cable.*—The variation of field with vertical height was measured for four different values of D/L, the results being plotted in figs. 6 and 7.

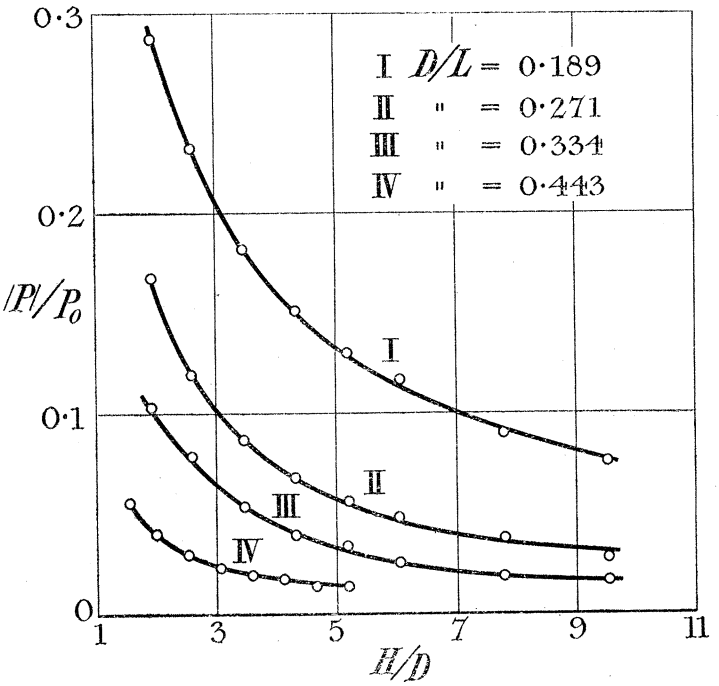

Fig. 6. Magnetic field vertically over cable.
|P| = Observed amplitude of field. H = Height above cable.
P_0 = Undisturbed field = 2I/H. D = Depth of lead.
L = Wave-length in lead = $\sqrt{\text{resistivity/frequency}}$.

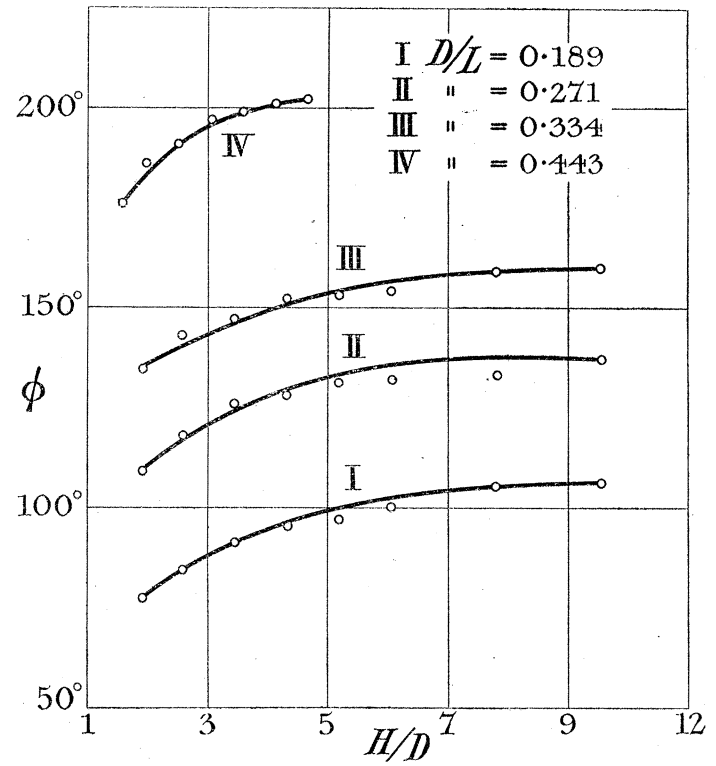

Fig. 7. Magnetic field vertically over cable.
ϕ = Angle of lag behind undisturbed field. H = Height above cable.
L = Wave-length in lead = $\sqrt{\text{resistivity/frequency}}$. D = Depth of lead.

For these values of D/L all we know from theory is the value of P/P_0 at the surface and at distant points. (See Chart 8, Plate 4, and equations (18) of Part 1.)

Equation (18) shows that if H be the height above the cable the value of $H/D \times P/P_0$ should tend to a constant value as H increases. This test has been applied in the table below, the results for H/D = 2, 4, 10, being obtained from the experimental curves, and those for H/D = 1, and infinity being those deduced from theory.

f = Frequency =	596		1230		1870		1230	
D = Depth (cm.) =	1·15		1·15		1·15		1·88	
L = $\sqrt{\rho/f}$ =	6·10		4·25		3·45		4·25	
$\frac{D}{L}$ =	0·189		0·271		0·334		0·443	
$\frac{H}{D}$	$\frac{H}{D}\frac{P}{P_0}$.	Phase.	$\frac{H}{D}\frac{P}{P_0}$.	Phase.	$\frac{H}{D}\frac{P}{P_0}$.	Phase.	$\frac{D}{H}\frac{P}{P_0}$.	Phase.
		°		°		°		°
1	0·465	56	0·302	84	0·214	106	0·115	146
2	0·56	77	0·33	110	0·20	136	0·080	186
4	0·64	93	0·30	120	0·18	150	0·072	202
10	0·72	106	0·29	136	0·14	160	—	—
Infinity	0·674	116	0·300	142	0·165	164	0·064	204

(B) *Points not vertically over the Cable.*—Seven traverses were made, the particulars of these traverses being given in the following table :—

Traverse No.	1.	2.	3.	4.	5.	6.	7.
Depth of lead— D cm.	1·15	1·15	1·15	1·15	1·88	1·15	1·88
Height above cable— H cm.	2·25	2·25	2·25	2·25	3·63	4·90	2·99
Frequency— ~ per second	596	950	1230	1870	1230	1230	1230
Wave-length in lead— L cm.	6·10	4·83	4·25	3·45	4·25	4·25	4·25
D/L	0·189	0·238	0·271	0·334	0·443	0·271	0·443
H/D	1·96	1·96	1·96	1·96	1·93	4·26	1·58

The results for a typical traverse are plotted in figs. 8 and 9. All the other traverses gave similar curves when plotted in this way. In fact when all the field amplitudes were expressed in terms of the actual central field (P_1), the resulting amplitude curves almost coincided when the abscissæ were x/H instead of x. Thus the mean values

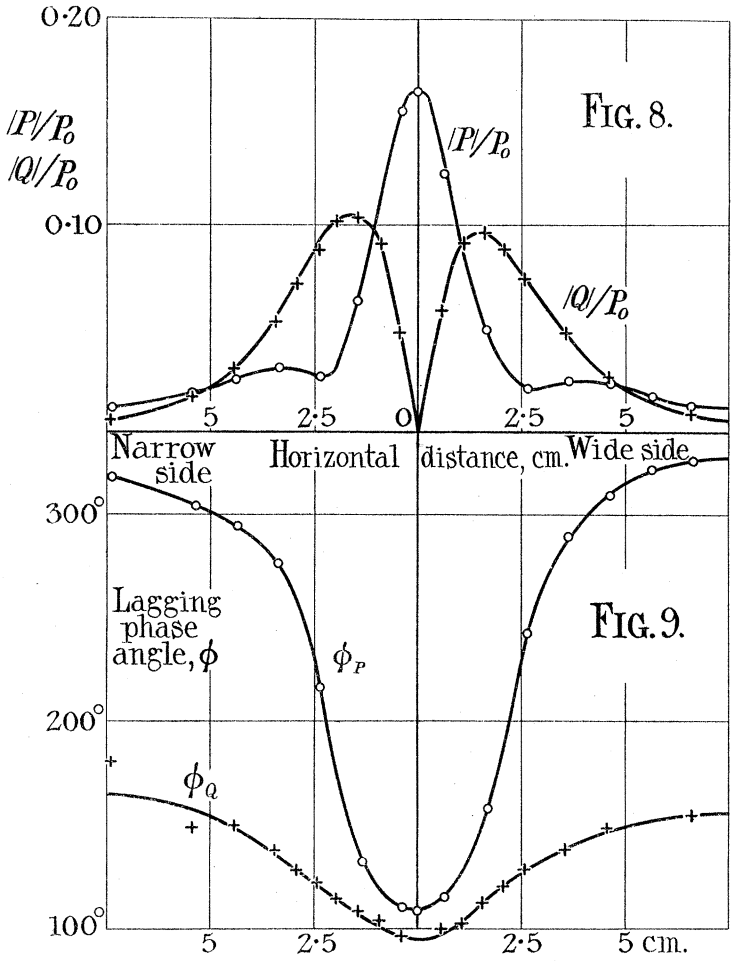

Figs. 8 and 9. Traverse No. 3.

Depth of lead = 1·15 cm. Frequency = 1230 ~ per sec.

Height above cable = 2·25 cm. Wave-length in lead = 4·25 cm.

P_0 = Undisturbed field vertically over cable.

$|Q|$ = Observed vertical field. $|P|$ Observed horizontal field.

(on either side the cable) of the maximum vertical field were the following fractions of the central horizontal field :—

$$\frac{Q_{max}}{P_1} = 0{\cdot}66 \quad 0{\cdot}66 \quad 0{\cdot}63 \quad 0{\cdot}63 \quad 0{\cdot}73 \quad 0{\cdot}70 \quad 0{\cdot}61$$

and their mean positions were given by

$$\frac{x}{H} = 0{\cdot}74 \quad 0{\cdot}68 \quad 0{\cdot}64 \quad 0{\cdot}66 \quad 0{\cdot}60 \quad 0{\cdot}66 \quad 0{\cdot}56$$

According to theory the value and position of Q_{max}/P_1 for large values of D/L or for large distances should be

$$Q_{max}/P_1 = 0{\cdot}650, \qquad x/H = 0{\cdot}577,$$

while at low frequencies or in the absence of the conducting sheet

$$Q_{max}/P_1 = 0{\cdot}500, \qquad x/H = 1{\cdot}00.$$

The phase angles when expressed with respect to P_1 also gave very similar curves on being plotted against x/H. In particular P and Q were in quadrature in the following positions :—

$$\frac{x}{H} = 1{\cdot}16 \quad 1{\cdot}06 \quad 1{\cdot}02 \quad 0{\cdot}94 \quad 0{\cdot}87 \quad 0{\cdot}88 \quad 0{\cdot}85.$$

The theory for large distances gives as the limiting position for this point $x = H$.

It will be noticed from fig. 8 that the curve representing the vertical field crosses that representing the horizontal field at four points, two on either side the cable. Denoting these points by x_1, x_2 and considering only one side, we have

$$x < x_1,\ P > Q\ ; \qquad x_1 < x < x_2,\ Q > P\ ; \qquad x_2 < x,\ P > Q.$$

Again if in fig. 9 x_3 is the point where P and Q are in quadrature—

$$x_1 < x_3 < x_2.$$

These properties are common to all the traverses and the points x_1, x_2, x_3 are important when the field is treated as an elliptically rotating field.

It may be shown that if ψ is the phase angle by which Q leads P, and α is the inclination of the axes of the elliptically rotating field,

$$\tan 2\alpha = \frac{2PQ \cos \psi}{P^2 - Q^2}$$

Thus when $P = Q$, the elliptic axes are at 45° and 135°. When $\psi = \pi/2$ the elliptic axes are at 0° and 90°. In the former case the amplitudes of the axes are

$$X = \sqrt{2}P \cos \psi/2, \qquad Y = \sqrt{2}P \sin \psi/2,$$

the phase of X being $\psi/2$ ahead of P. In the latter case the amplitudes are of course P and Q. Paying regard to the phase difference ψ we therefore have the following sequence :—

$x = 0$	Field horizontal and linear.
$0 < x < x_1$	Field elliptic. Inclination of major axis $< 45°$.
$x = x_1$	Major axis at 45° and equal to $\sqrt{2}P \cos \psi/2$. Ratio of axes = $\tan \psi/2$. Phase of major axis = $\phi_P - \psi/2$ behind current.
$x_1 < x < x_3$	Major axis $> 45°$ and $< 90°$.
$x = x_3$	Major axis vertical, phase = ϕ_Q. Amplitude = Q. Ratio of axes = P/Q.
$x_3 < x < x_2$	Major axis $> 90°$ and $< 135°$.
$x = x_2$	Major axis at 135°. Phase = $\phi_Q + \psi/2 - 90°$. Amplitude = $\sqrt{2}P \sin \psi/2$. Ratio of axis = $\cot \psi/2$.
$x > x_2$	Major axis $> 135°$ and $< 180°$.

The following results have been deduced from the observations of the various traverses.

Elliptic fields producing measured field components :—

H = height above cable.
x = horizontal distance.
ρ = actual distance.
D = depth of lead.
θ = angular distance from vertical.
X_0 = undisturbed field at x.
X = amplitude of major axis.
Y = amplitude of minor axis.
α = inclination of major axis.
χ = phase lag of major axis behind cable current.

Traverse.	$\frac{H}{D}$.	$\frac{D}{L}$.	$\frac{x}{H}$.	θ.	$\frac{\rho}{D}$.	α.	$\frac{X}{X_0}$.	$\frac{Y}{X}$.	χ.	$\frac{\rho}{D} \cdot \frac{X}{X_0}$.
1	1·96	0·189	0	° 0	1·96	° 0	0·288	0	° 78	0·56
			0·48	26	2·18	45	0·267	0·14	80	0·63
			1·16	48	3·00	90	0·240	0·38	89	0·74
			2·38	67	5·06	135	0·206	0·25	100	1·02
			Infinity	—	—	—	—	—	(116)	(0·67)
2	1·96	0·238	0	0	1·96	0	0·198	0	95	0·39
			0·49	26	2·18	45	0·173	0·17	99	0·38
			1·06	47	2·86	90	0·156	0·34	110	0·44
			2·30	67	4·90	135	0·080	0·29	133	0·43
			Infinity	—	—	—	—	—	(131)	(0·41)
3	1·96	0·271	0	0	1·96	0	0·164	0	109	0·32
			0·48	26	2·18	45	0·143	0·19	113	0·31
			1·02	46	2·80	90	0·126	0·30	115	0·35
			2·30	67	4·90	135	0·062	0·24	143	0·30
			Infinity	—	—	—	—	—	(142)	(0·30)
4	1·96	0·334	0	0	1·96	0	0·102	0	135	0·20
			0·46	25	2·16	45	0·090	0·13	140	0·19
			0·94	43	2·68	90	0·078	0·25	145	0·21
			2·04	64	4·45	135	0·051	0·15	158	0·23
			Infinity	—	—	—	—	—	(164)	(0·165)
5	1·93	0·443	0	0	1·93	0	0·0398	0	187	0·077
			0·38	21	2·06	45	0·0376	0·18	189	0·077
			0·87	41	2·55	90	0·0324	0·25	200	0·083
			>2	—	—	135	—	—	—	—
			Infinity	—	—	—	—	—	(204)	(0·064)
6	4·26	0·271	0	0	4·26	0	0·069	0	128	0·29
			0·40	22	4·60	45	0·062	0·09	130	0·29
			0·88	41	5·67	90	0·057	0·14	133	0·32
			2·30	67	10·63	135	0·029	0·05	143	0·30
			Infinity	—	—	—	—	—	(142)	(0·30)
7	1·58	0·443	0	0	1·58	0	0·056	0	176	0·088
			0·40	22	1·71	45	0·0475	0·14	184	0·081
			0·85	40	2·07	90	0·0375	0·35	197	0·072
			2·0	64	3·54	135	0·0190	0·12	222	0·067
			Infinity	—	—	—	—	—	(204)	(0·064)

The angles in the column headed " θ " are the angular directions at which the elliptic field is inclined at 0°, 45°, 90°, 135° to the horizontal. According to the " distant field " theory these angles should settle down to the values 0°, 22·5°, 45°, 67·5°. It is seen that the observed directions are never more than 5° from these theoretical directions.

The magnitudes of the major axes divided by the magnitude of the undisturbed field are given in column 8. This ratio may be taken as the " reduction factor " at the point in question. It is seen that the reduction factor falls continually as we recede from the cable. Theory indicates that the reduction factor should be such that $\frac{\rho}{D} \cdot \frac{X}{X_0}$ tends to a constant value as the distance ρ increases. This test is applied in the last column, the theoretical value being given at the foot of the column. The values of $\frac{\rho}{D} \cdot \frac{X}{X_0}$ are fairly constant for each traverse and of the same order as the theoretical limiting value. The constancy of $\frac{\rho}{D} \cdot \frac{X}{X_0}$ indicates that the field is varying inversely as the square of distance since X_0 varies inversely as the distance.

The ellipticity of the field as measured by the ratio of the minor to the major axis is given in column 9. It is seen that it is greatest in the neighbourhood of the vertical field and increases on approaching the surface. There appears to be a diminution with increase of D/L at a constant vertical height. The maximum recorded ellipticity is 0·38, when D/L = 0·19.

The phase lag χ is given in column (9). This angle appears in general to be tending satisfactorily towards the limiting theoretical value. The whole change of phase is not large and becomes less as D/L increases for a given vertical height. This again is in accordance with theory, which shows that at low frequencies the whole phase change from the surface point vertically over the cable to distant points is 90°, while at high frequencies it is 45°, and further shows that the region of application of the " distant " theory approaches the surface point as the frequency increases.

The following table compares reduction factors and phase angles with the corresponding quantities at the vertical point as read off from figs. 6 and 7.

Traverse No.	$\frac{D}{L}\cdot$	$\frac{\rho}{D}\cdot$	θ.	$\frac{X_0}{X}$ at θ, ρ.		$\frac{X_0}{X}$ at 0, ρ.		Traverse No.	$\frac{D}{L}\cdot$	$\frac{\rho}{D}\cdot$	θ.	$\frac{X_0}{X}$ at θ, ρ.		$\frac{X}{X_0}$ at 0, ρ.	
				Amp.	Phase.	Amp.	Phase.					Amp.	Phase.	Amp.	Phase.
1	0·19	2·18	26°	0·267	80°	0·267	80°	4	0·33	2·16	25°	0·098	140°	0·092	138°
		3·00	48	0·240	89	0·208	87			2·68	43	0·078	145	0·074	142
		5·06	67	0·206	100	0·132	98			4·45	64	0·051	158	0·039	152
3	0·27	2·18	26	0·143	113	0·154	112	5	0·44	2·06	21	0·038	189	0·038	186
		2·80	46	0·126	115	0·111	120			2·55	41	0·032	200	0·029	193
		4·90	67	0·062	143	0·061	131								
6	0·27	4·60	22	0·062	130	0·065	130	7	0·44	1·71	22	0·048	184	0·050	179
		5·67	41	0·057	133	0·051	133			2·07	40	0·038	197	0·038	186
		10·63	67	0·029	143	0·025	137			3·54	64	0·019	222	0·020	200

This table shows that we are not far from the truth if we assume that the amplitude and phase of the field are functions only of distance and not of direction.

III. Comparison of Theory with Sea-Observations.

1. An exhaustive research on the field distribution above a submarine cable carrying alternating currents has been carried out by Dr. C. V. Drysdale on the Gareloch.* I am indebted to him for having access to his experimental results before publication. The cable used was a twin core armoured cable, each core consisting of 19/24 copper wire and armoured with 22 No. 12 steel wires, the external diameter of the cable being approximately 1 inch. Its length was about 3 miles, its distance from the eastern shore of the loch was about 300 yards, the whole width of the loch being about 1500 yards in the region of the observations and the depth of immersion of the cable about 72 feet. In the discussion of the results it is sometimes necessary to distinguish between observations on the shore side of the cable and observations in the region beyond the cable. These two regions are denoted in the succeeding tables by " S " and " F " respectively.

It is also necessary to consider the absorption of energy, by the cable armouring as the observed fields will differ from the undisturbed field due to the current in the cable core not only because of the distorting effect of the sea-water but also because of the eddy currents induced in the armouring of the cable. In order to distinguish between these two effects Dr. Drysdale measured the effective current producing the field outside the cable sheath and expressed all his results in terms of this current.

The corrections to be applied to the core current in order to allow for the effect of the armour are given in the following table :—

Frequency ~ per second.	Effective Current / Core Current.			
	Experimental.		Theoretical.	
	Amplitude.	Phase Lag.	Amplitude.	Phase Lag.
		°		°
15	0·78	16	1·00	10
50	0·59	39	0·89	34
120	0·45	50	0·60	60
250	0·30	61	0·33	77
500	0·17	76	0·18	82

The theoretical results have been calculated from the dimensions of the cable by the method of Oldenburg.† It is important to notice the large discrepancy between theory and observation at the lower frequencies.

* See preceding paper.

† 'Archiv fur Elecktrotechnik,' IX, vol. 7, p. 289 (1920).

2. *Observations above the Surface of the Sea.*

The amplitude and phase of the horizontal and vertical components of the field were measured at heights of approximately 35, 20 and 10 feet above the surface, the observations covering a range of approximately 200 yards on either side the cable. From these observations the nature of the elliptically rotating field was deduced for each point. Measurements were made for five different frequencies, viz. :—15, 50, 120, 250 and 500 cycles per second, and as about 50 points were taken for each frequency there are about 250 groups of observations available for comparison for theory.

However, since the accuracy of observation naturally falls off as we recede from the cable and as a point by point comparison would involve too much labour, a system of averaging has been adopted.

Let X = major field, Y = minor field.

α = inclination of major axis to horizontal.

ϕ = phase lag of X behind effective current at a point distance ρ from the cable and inclined at an angle θ.

Also let X_0 = undisturbed field calculated from

$$X_0 = 2I/\rho,$$

where I is the effective current.

Then the ratio X/X_0 tells us how much the field is reduced at any point, and will therefore be referred to as the reduction factor (R).

Y/X measures the ellipticity of the field (E).

The two quantities R and E together with the inclination α and the phase lag ϕ give the simplest possible complete specification of the field. With the exception of certain observations at a frequency of 120 cycles per second and on the shore side of the cable, both theory and experiment agree in the following main properties of the field throughout the range of observations :—

(1) The reduction factor R is almost independent of position.

(2) The ellipticity E increases almost uniformly up to about $\theta = 60°$, then passes through a maximum and falls to zero at large distances.

(3) The major axis of the field passes from horizontal to vertical and then tends to become horizontal again as we proceed horizontally outwards. Throughout this change α increases almost uniformly with θ.

(4) The change of phase is small until θ exceeds 60° and then tends to a constant value at large distances.

The following tables illustrate the above properties and afford a quantitative comparison between theory and observation :—

REDUCTION FACTOR.

Experimental.					Theoretical.				
Frequency.	Depth.	Height.	Central R.	Mean R.	Depth.	Height.	$x = 0$.	50 Metres.	100 Metres.
	Feet.	Feet.			Feet.	Feet.			
15	70	33	1·17	1·13 S 1·12 F					
	71	20	1·18	1·11 S 1·33 F	72	25	0·84	0·83	0·80
	73	12	1·35	1·31 S 1·28 F					
50	76	33	0·94	0·93 S 1·07 F					
	76	20	1·12	0·90 S 1·04 F	72	25	0·65	0·60	0·51
	74	9	1·21	1·10 S 1·16 F					
120	74	35	0·56	0·84 S 0·55 F					
	77	20	0·58	0·67 S 0·58 F	72	25	0·47	0·34	0·25
	76	10	0·67	1·01 S 0·76 F					
250	75	36	0·42	0·45 S 0·35 F					
	75	20	0·45	—	72	25	0·33	—	—
	70	10	0·57	0·51 S 0·49 F					
500	78	35	0·16	0·17 S 0·18 F					
	70	20	0·22	0·24 S 0·25 F	72	25	0·22	—	—
	77	10	0·22	0·33 S 0·25 F					

The observations as they stand indicate that the field is strengthened instead of weakened at the lower frequencies. If, however, we make use of the armouring

corrections and multiply the experimental reduction factor R for the sea by the experimental reduction factor Ra for the armouring and the theoretical reduction factor for the sea by the theoretical reduction factor for the armouring we obtain the following central values :—

Frequency	= 15	50	120	250	500
Whole reduction factor—					
Theoretical	= 0·84	0·58	0·28	0·11	0·040
Observed	= 0·92	0·66	0·26	0·135	0·036

and the discrepancy has almost disappeared.

Now the experimental correction has cancelled out the experimentally observed armouring effects so from this it appears that the abnormal results at the lower frequencies may be due to some error in determining the reduction due to the armouring.

ELLIPTICITY.

Frequency.	Experimental. Mean E.	Theoretical. Max. E.	
		Value.	Angular Position.
			°
15	0·23	0·51	86
50	0·22	0·43	78
120	0·14	0·36	70
250	0·27	—	—
500	0·36	—	—

Here the mean values are taken over all the traverses as the individual variations did not permit more refined treatment. It is seen that the mean ellipticities are approximately half the theoretical maxima and as the latter all occur on the outer fringe of the observations, theory and experiment are in agreement.

Inclination of Major Axis.

The observations indicated almost a straight line law for α when plotted against angular position θ. The slope of the curve is fixed by the point where the ellipse is vertical.

Frequency	= 15	50	120	250	500
Angular position of vertical ellipse—					
Theoretical	68°	62°	52·5°	—	—
Experimental	67°	63°	51°	44°	29°

The straight line law cannot hold, however, for all distances, as according to theory the value of α should tend to 180° at θ=90° for all frequencies. However, the region of pronounced curvature lies outside the range of observation.

Phase Lag of Major Axis of Elliptic Field.

The results have been treated in the same way as those for the reduction factor. The table gives the observed phases vertically over the cable and the mean values of the phases measured on the shore side (S) and the far side (F). On the theoretical side the central phase and the ultimate phase angle distant points are given, while the manner in which the phase changes from the vertical point is indicated by calculating the phase at the point where the elliptic field is vertical. These results are entered in the column headed ϕ_v.

The heights and depths to which these results correspond are given in the Reduction Factor table above.

PHASE LAG ϕ.

Frequency.	Experimental.		Theoretical.		
	ϕ Central.	ϕ Mean.	ϕ Central.	ϕ_v.	ϕ Ultimate.
15	° 6	° 4 S, 17 F	° 15	° 19	° 92
	7	10 S, 13 F			
	8	8 S, 18 F			
50	12	45 S, 22 F	30	44	97
	16	45 S, 39 F			
	12	38 S, 26 F			
120	40	225 S, 92 F	44	54	107
	43	181 S, 73 F			
	45	164 S, 61 F			
250	52	63 S, 61 F	66	—	125
	62	—			
	68	68 S, 72 F			
500	90	84 S, 101 F	96	—	151
	94	92 S, 100 F			
	140	106 S, 129 F			

The tables in general show that the agreement between theory and observation is fairly good except in the case of the results at a frequency of 120 cycles. In this case there is a remarkable asymmetry in the field, the distribution on the shore side being quite abnormal.

In all three traverses the observations on the shore side of the cable gave a stronger field, a more rapid change of phase and inclination and a marked reduction in ellipticity as compared with corresponding observations on the far side of the cable. In two of the traverses the field actually increased as the shore was approached and always the field was stronger than that due to a cable at a corresponding distance in free air. All these phenomena appear to point to some disturbance in the neighbourhood of the shore and above the surface of the sea.

3. *Observations below the Surface of the Sea.*

Below the surface of the sea the observations included not only the magnitude of the field, but also the amplitude and phase of the current density. Theory can only be applied for points vertically above the cable.

The comparisons are given in the following tables :—

MAGNETIC FIELD.

Frequency.	Depth.	Height above Cable.	Experimental.		Theoretical.	
			$\frac{X}{X_0}$.	ϕ.	$\frac{X}{X_0}$.	ϕ.
	Feet.	Feet.		°		°
15	72	44	1·27	0	1·09	4
		52	1·27	4	1·09	7
		65	1·33	6	1·11	9
50	75	44	1·92	6	1·10	7
		55	1·44	0	1·05	10
		68	1·30	6	0·85	18
120	75	45	1·10	15	1·02	12
		55	0·96	22	0·88	18
		70	0·84	35	0·68	33
250	72	42	1·41	10	0·95	20
		52	1·01	20	0·83	27
		68	0·62	40	0·52	50
500	76	46	0·98	40	0·82	40
		56	0·97	40	0·67	51
		71	0·43	72	0·37	77

X = Actual field.
X_0 = Undisturbed field.
ϕ = Phase lag of field behind effective cable current.

CURRENT DENSITY.

Frequency.	Depth.	Height above Cable.	Experimental.		Theoretical.	
			$\frac{i}{I} \times 10^8$.	ϕ.	$\frac{i}{I} \times 10^8$.	ϕ.
	Feet.	Feet.		°		°
15	72	44	2·3	117	2·6	108
		52	2·2	120	2·6	111
		65	1·8	124	2·0	114
50	75	44	5·3	113	4·4	123
		55	4·2	122	4·0	130
		68	3·5	127	3·3	133
120	75	45	6·3	140	6·3	138
		55	5·0	147	5·5	148
		70	4·6	155	4·3	155
250	72	42	8·9	140	8·8	152
		52	7·8	154	7·2	164
		68	3·9	164	5·8	177
500	76	46	8·9	172	9·1	177
		56	8·1	181	7·3	193
		71	4·9	204	5·7	211

i = current density in sea (amperes per sq. cm.).
I = effective cable current (amperes).
ϕ = phase lag of i behind I.

The agreement in regard to phase and current density is good, but all the observed fields are greater than the theoretical ones.

It should be noted that agreement in regard to field can be obtained if the experimental armouring corrections are replaced by the theoretical ones, but this alteration would cause the theoretical and experimental current densities to disagree.

APPENDIX.—TABLES.

TABLE I.—Wave-length (L) of electro-magnetic waves in sea-water of resistivity 25 ohms. per cm. cubes.

Frequency ∽ per second .	10	20	50	100	250	500	1000	2000
Wave-length (metres) . .	500	354	224	158	100	71	50	35

TABLE II.—Field at points vertically over cable. $D/L < 0{\cdot}2$.

D = Depth of sea. L = Wave-length in sea. P_I = Quadrature component of field.
H = Height above cable. $\beta = 4\pi^2 DH/L^2$. P_0 = Undisturbed field at height H.
P_R = In-phase component of field. ϕ = Lag of P behind P_0.

β.	P_R/P_0.	$-P_I/P_0$.	$\lvert P\rvert/P_0$.	ϕ.
0·0	1·0000	0	1·000	0°
0·1	0·8709	0·1866	0·891	12·1
0·2	0·7726	0·2588	0·815	18·5
0·3	0·6928	0·2989	0·751	23·3
0·4	0·6262	0·3225	0·704	27·2
0·5	0·5696	0·3364	0·662	30·6
0·6	0·5209	0·3439	0·624	33·4
0·7	0·4784	0·3473	0·590	36·0
0·8	0·4410	0·3478	0·561	38·3
0·9	0·4080	0·3463	0·535	40·3
1·0	0·3786	0·3434	0·512	42·2
2·0	0·2020	0·2891	0·353	55·1
3·0	0·1241	0·2378	0·268	62·4
4·0	0·0832	0·1987	0·216	67·2
5·0	0·0593	0·1695	0·180	70·6
6·0	0·0442	0·1472	0·153	73·3
7·0	0·0340	0·1297	0·135	75·3
8·0	0·0270	0·1157	0·119	76·8
9·0	0·0218	0·1043	0·106	78·2
10·0	0·0183	0·0949	0·096	79·1

TABLE III.—Field on surface of lamina. $D/L < 0{\cdot}2$.

Q_0 = Undisturbed field. Q_R = In-phase component of vertical field.
Q_I = Quadrature component of vertical field.
P_R = In-phase component of horizontal field.
P_I = Quadrature component of horizontal field.
$\alpha = 4\pi^2 Dx/L^2$ = horizontal distance from cable.

α.	Q_R/Q_0.	$-Q_I/Q_0$ $+P_R/Q_0$.	P_I/Q_0.	α.	Q_R/Q_0.	$-Q_I/Q_0$ $+P_R/Q_0$.	P_I/Q_0.
0·1	+0·973	+0·142	+0·174	2·0	−0·032	+0·425	−0·309
0·2	0·916	0·257	0·214	2·2	0·068	0·382	0·330
0·3	0·865	0·349	0·217	2·4	0·096	0·341	0·346
0·4	0·796	0·421	0·196	2·6	0·118	0·304	0·351
0·5	0·700	0·476	0·162	2·8	0·129	0·266	0·353
0·6	0·625	0·517	0·122	3·0	0·135	0·234	0·348
0·7	0·551	0·546	0·078	4·0	0·132	0·115	0·308
0·8	0·481	0·565	+0·034	5·0	0·100	0·053	0·250
0·9	0·415	0·575	−0·009	6·0	0·076	0·023	0·204
1·0	0·353	0·578	0·050	7·0	0·051	0·010	0·171
1·2	0·244	0·567	0·125	8·0	0·040	0·004	0·143
1·4	0·151	0·543	0·185	9·0	0·031	0·002	0·123
1·6	0·075	0·509	0·242	10·0	−0·023	+0·001	−0·108
1·8	+0·014	0·468	0·281				
2·0	−0·032	+0·425	−0·309				

PHILOSOPHICAL TRANSACTIONS OF THE ROYAL SOCIETY A MATHEMATICAL, PHYSICAL & ENGINEERING SCIENCES

Field at Points not vertically over Cable. $D/L < 0{\cdot}2$.

r = Distance from cable.
θ = Inclination of r to vertical.
H_0 = Amplitude if undisturbed field at r, θ.
P_R = In-phase component of horizontal field.
Q_R = In-phase component of vertical field.
P_I = Quadrature component of horizontal field.
Q_I = Quadrature component of vertical field.
$R = 4\pi^2 Dr/L^2$.
D = Depth of sea.
L = Wave-length in sea = $\sqrt{\text{resistivity/frequency}}$.

Table IV.—P_R/H_0.

R =	1	2	3	4	5	6	7	8	9	10
θ °										
0	0·3786	0·2020	0·1241	0·0832	0·0593	0·0442	0·0340	0·0270	0·0219	0·0181
15	0·3457	0·1756	0·1040	0·0676	0·0470	0·0344	0·0261	0·0205	0·0164	
30	0·2494	0·1004	0·0470	0·0243	0·0136	0·0081	0·0051	0·0033	0·0022	0·0016
45	0·0967	−0·0154	−0·0367	−0·0363	−0·0312	−0·0258	−0·0212	−0·0174	−0·0145	
60	−0·1018	−0·1562	−0·1297	−0·0971	−0·0717	−0·0535	−0·0408	−0·0322	−0·0258	−0·020
75	−0·3314	−0·3025	−0·2071	−0·1339	−0·0869	−0·0580	−0·0405	−0·0280	−0·0288	
90	−0·5776	−0·4252	−0·2347	−0·1151	−0·0529	−0·0233	−0·0100	−0·0042	−0·0017	−0·0007

Table V.—P_I/H_0.

R =	1	2	3	4	5	6	7	8	9	10
θ °										
0	−0·3434	−0·2891	−0·2377	−0·1987	−0·1695	−0·1472	−0·1296	−0·1157	−0·1045	−0·0949
15	−0·3338	−0·2740	−0·2209	−0·1820	−0·1536	−0·1322	−0·1157	−0·1028	−0·0921	
30	−0·3047	−0·2282	−0·1707	−0·1327	−0·1069	−0·0888	−0·0758	−0·0656	−0·0583	−0·0542
45	−0·2548	−0·1505	−0·0873	−0·0526	−0·0331	−0·0217	−0·0148	−0·0104	−0·0075	
60	−0·1768	−0·0383	0·0286	0·0540	0·0611	0·0608	0·0577	0·0538	0·0496	0·047
75	−0·0820	0·1127	0·1754	0·1788	0·1632	0·1439	0·1262	0·112	0·099	
90	0·0504	0·3092	0·3487	0·3065	0·2508	0·203	0·168	0·142	0·122	0·108

PHILOSOPHICAL TRANSACTIONS OF THE ROYAL SOCIETY A MATHEMATICAL, PHYSICAL & ENGINEERING SCIENCES

TABLE VI.—Q_R/H_0.

R =	1	2	3	4	5	6	7	8	9	10
θ °										
0	0	0	0	0	0	0	0	0	0	0
15	−0·1685	−0·1070	−0·0720	−0·0510	−0·0376	−0·0287	−0·0225	−0·0181	−0·0148	
30	−0·3169	−0·1934	−0·1254	−0·0860	−0·0618	−0·0461	−0·0355	−0·0281	−0·0227	−0·0207
45	−0·4259	−0·2397	−0·1431	−0·0910	−0·0612	−0·0432	−0·0318	−0·2420	−0·0189	
60	−0·4831	−0·2279	−0·1109	−0·0563	−0·0299	−0·0167	−0·0097	−0·0059	−0·0034	−0·003
75	−0·4582	−0·1421	−0·0193	+0·0210	+0·0300	+0·0288	+0·0248	+0·021	+0·017	
90	−0·3532	+0·0318	+0·1352	+0·1318	+0·1028	+0·0750	+0·0539	+0·040	+0·030	+0·024

TABLE VII.—Q_I/H_0.

R =	1	2	3	4	5	6	7	8	9	10
θ °										
0	0	0	0	0	0	0	0	0	0	0
15	0·0990	0·1050	0·0962	0·0855	0·0758	0·0676	0·0607	0·0548	0·0499	
30	0·1975	0·2052	0·1843	0·1611	0·1408	0·1240	0·1103	0·0989	0·0895	0·0816
45	0·2949	0·2954	0·2553	0·2159	0·1836	0·1582	0·1382	0·1224	0·1095	
60	0·3908	0·3687	0·2984	0·2376	0·1921	0·1591	0·1347	0·1162	0·1021	0·092
75	0·4856	0·4164	0·2987	0·2106	0·1531	0·1164	0·0923	0·077	0·064	
90	0·5776	0·4252	0·2347	0·1151	0·0529	0·0233	0·0100	0·0042	0·0017	0·0007

Note in regard to Signs.—In Tables IV. to VII. H_0 is signless, and the conventional positive directions of the various components are those shown in fig. 1. The signs in the tables refer to the case in which the undisturbed field vertically over the cable is in the positive direction, that is the case in which the cable current is reckoned positive when flowing *inwards* in fig. 1. The convention makes Q_0 negative in Table III. and thus accounts for the discrepancy in sign in Table III. θ is positive when rotation is from Oy to Ox in fig. 1. Q is an odd function and P an even function of θ.

PHILOSOPHICAL TRANSACTIONS OF THE ROYAL SOCIETY A MATHEMATICAL, PHYSICAL & ENGINEERING SCIENCES

Field and Electric Force below the Surface of the Sea. $D/L > 0{\cdot}25$.

Table VIII.—(See Equations 57.)

ξ, or ξ'.	$E_1/4j\omega I_0$.		$E_2/4j\omega I_0$,		$P_1/4j\Lambda I_0$.		$P_2/4j\Lambda I_0$.	
	Real.	Imag.	Real.	Imag.	Real.	Imag.	Real.	Imag.
0·5	+0·579	−0·402			−0·813	−0·677		
1·0	+0·216	−0·3233			−0·459	−0·199		
1·5	+0·0530	−0·2291			−0·282	−0·024		
2·0	−0·0200	−0·1479			−0·1661	+0·0410		
2·5	−0·0456	−0·0850			−0·0898	+0·0595		
3·0	−0·0475	−0·0416	−0·0416	−0·0267	−0·0416	+0·0556	+0·0277	−0·0234
3·5	−0·0391	−0·0148	−0·0205	−0·0119	−0·0131	+0·0434	+0·0119	−0·0216
4·0	−0·0279	−0·00017	−0·0160	−0·0026	+0·0016	+0·0299	+0·00235	−0·01674
4·5	−0·01754	+0·00640	−0·01088	+0·00218	+0·00787	+0·01832	−0·00252	−0·01129
5·0	−0·00957	+0·00816	−0·00648	+0·00405	+0·00915	+0·00969	−0·00434	−0·00664
5·5	−0·00414	+0·00742	−0·00318	+0·00418	+0·00803	+0·00400	−0·00438	−0·00323
6·0	−0·00088	+0·00570	−0·00103	+0·00347	+0·00602	+0·00670	−0·00360	−0·00103
6·5	+0·000779	+0·00381	+0·00016	+0·00249	+0·00399	−0·00098	−0·00257	+0·00021
7·0	+0·001411	+0·00227	+0·000702	+0·001570	+0·00231	−0·00156	−0·001605	+0·000753
7·5	+0·001441	+0·001117	+0·000835	+0·000847	+0·001109	−0·001541	−0·000859	+0·000875
8·0	+0·001190	+0·000373	+0·000746	+0·000346	+0·000346	−0·001248	−0·000345	+0·000771
8·5	+0·000853	−0·000029	+0·000567	+0·000044	−0·000073	−0·000882	−0·000037	+0·000583
9·0	+0·000538	−0·000231	+0·000379	−0·000108	−0·000256	−0·000549	+0·000117	+0·000386
9·5	+0·000291	−0·000277	+0·000219	−0·000162	−0·000295	−0·000293	+0·000169	+0·000222
10·0	+0·0001216	−0·000248	+0·000103	−0·000158	−0·000259	−0·000118	+0·000163	+0·000103